Naval R...
Rev...

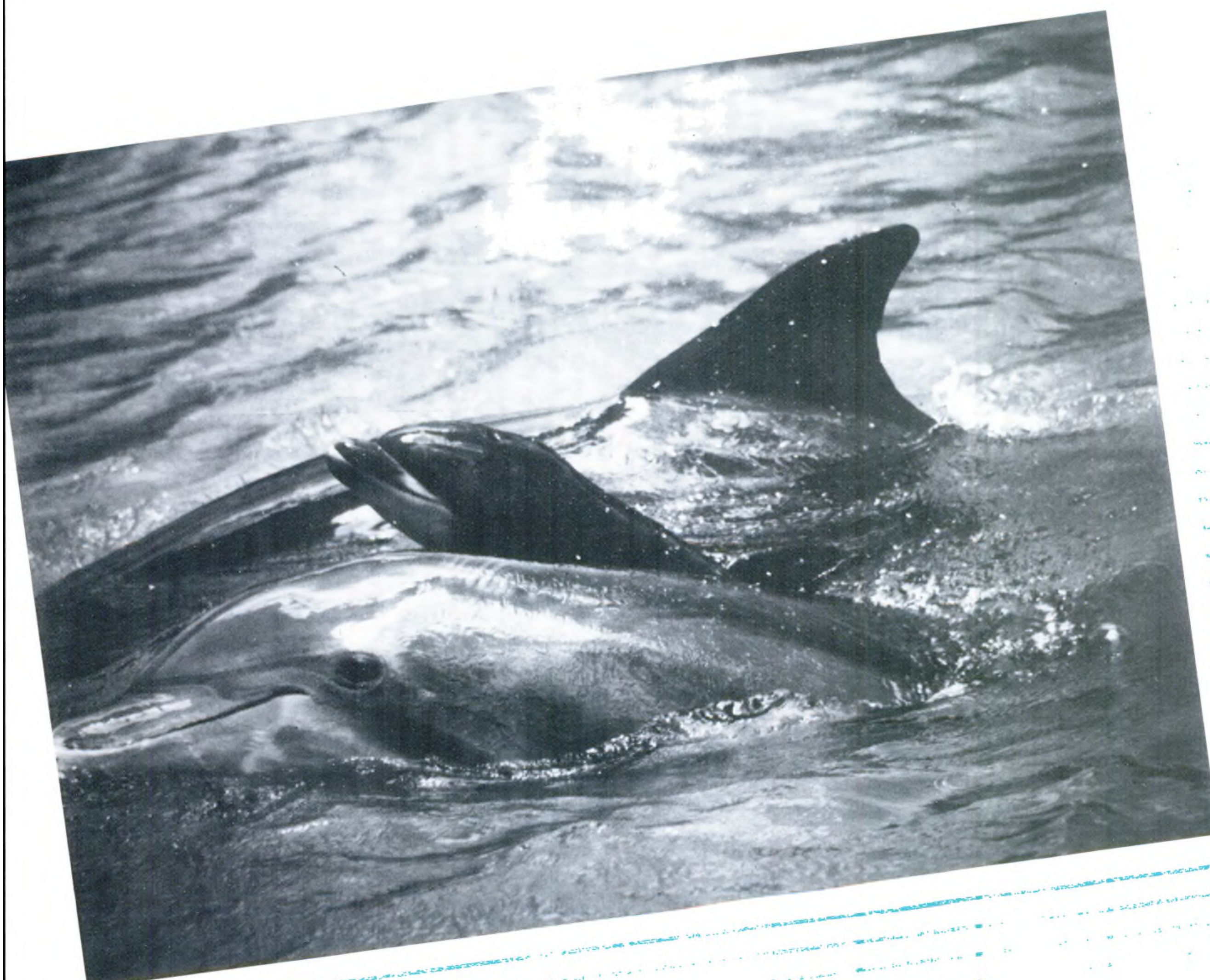

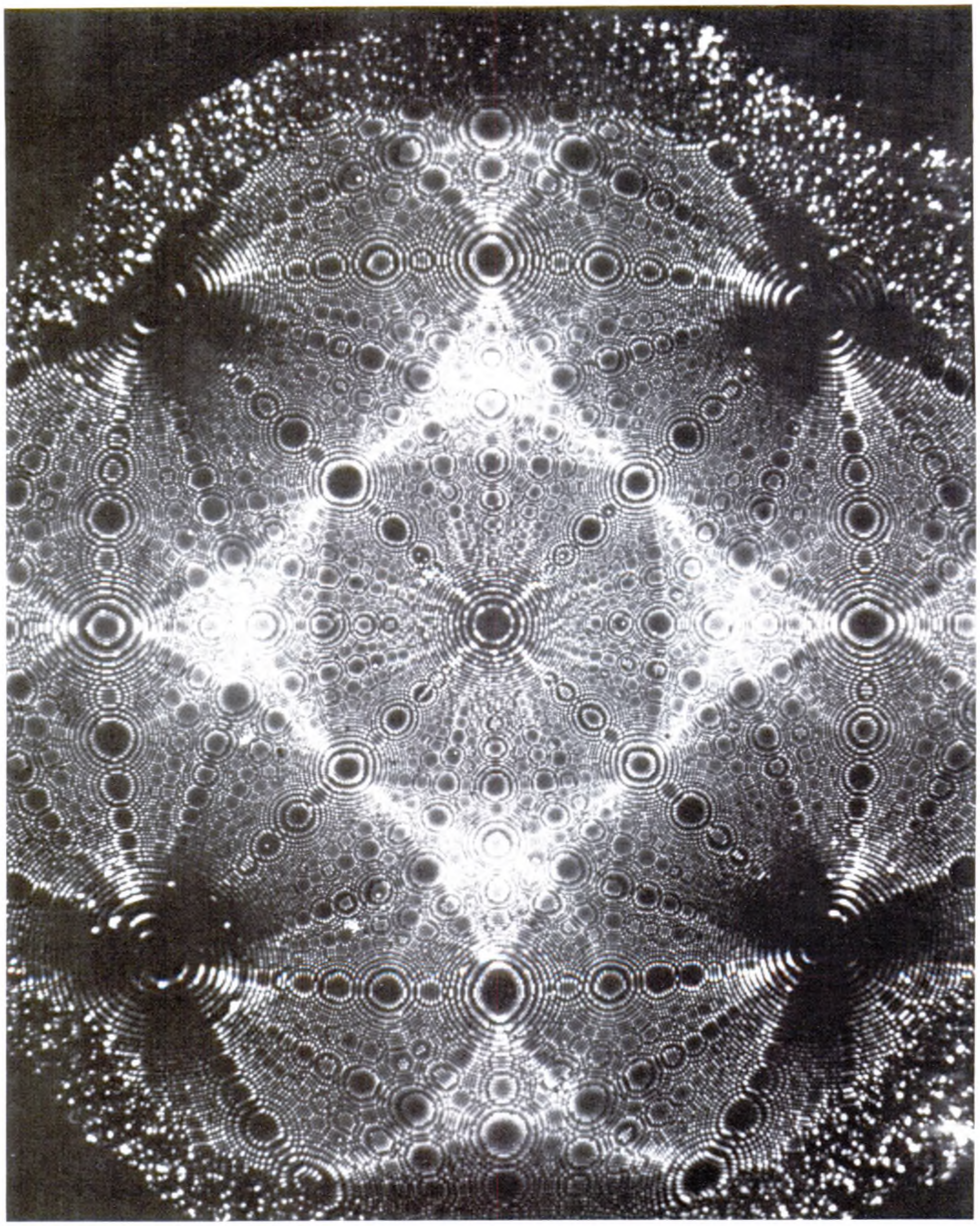

Field Ion Microscope

A field-ion microscope picture of a platinum single crystal surface taken by the late Professor Erwin W. Mueller of Pennsylvania State University in the early 1960's. The picture shows the arrangement of surface atoms after field evaporation. Mueller invented the field-ion microscope in 1951 at the Fritz Haber Institute, Germany. In 1952 Mueller went to Pennsylvania State University where he significantly improved the resolution of the microscope with funding from the Office of Naval Research. Further understanding of the image formation and the processes of field ionization, field evaporation, and field adsorption of gases was achieved mostly through the work of Mueller and his long-time colleague, Professor T. T. Tsong of Pennsylvania State University. The field-ion microscope together with the technique of controlled field desorption, made it possible to study atomic processes on atomically perfect surfaces in microscopic detail and also led to the development of field ionization mass spectrometry as an analytical tool.

Naval Research Reviews

Office of Naval Research
Two / 1989
Vol XLI

Articles

Departments

About the Cover

Baby bottlenose Atlantic dolphin being supported by mother and helper. Sometimes, young dolphin need to be brought to the surface for air in this manner. (See article on page 2)

Naval Research Reviews publishes articles about research conducted by the laboratories and contractors of the Office of Naval Research and describes important naval experimental activities. Manuscripts submitted for publication, correspondence concerning prospective articles, and changes of address, should be directed to Code OPARI, Office of Naval Research, Arlington, VA 22217-5000. Requests for subscriptions should be directed to the Superintendent of Documents, U.S. Government Printing Office, Washington, DC 20403. *Naval Research Reviews* is published from appropriated funds by authority of the Office of Naval Research in accordance with Navy Publications and Printing Regulations. NAVSO P-35.

Investigation of the 1987 - 1988 Mass Mortality of the Bottlenose Dolphin*

by J. R. Geraci, University of Guelph, Ontario, Canada

Introduction

From early June, 1987, until March, 1988, unprecedented numbers of bottlenose dolphins, *Trusiops truncatus*, washed ashore along the Atlantic coast from New Jersey to Florida. The event was unparalleled, and therefore demanded a comprehensive investigation of proximate and contributing factors. Routine laboratory protocols were modified to meet rigorous research standards. Contributing laboratories with expertise in pathology, biochemistry, microbiology, virology, contaminants, and biotoxins performed analyses on coded samples from the dolphins. Specimens for contaminant and biotoxin analysis were mixed with controls from unrelated *Tursiops* and four other cetacean species. At the termination of each study, data were transferred to our laboratory at the University of Guelph, Canada and integrated with identifying information. The investigation shows that the dolphins apparently were poisoned by brevetoxin, a neurotoxin produced by the dinoflagellate *Ptychodiscus brevis,* Florida's red tide organism. The dolphins were eventually infected with a host of bacterial and viral pathogens which produced an array of beguiling clinical signs.

Specimen Collection

Over 740 bottlenose dolphins stranded along the Atlantic coast during the 11-month period beginning June, 1987.[1] Data or specimens from 347 of these were available for analysis by the investigating team. Studies on pathology, virology, microbiology, and chemical and biological toxicology were carried out only on freshly dead animals (Table 1).

To examine and obtain blood samples from live animals, four bottlenose dolphins were captured just offshore along Virginia Beach on August 16, and nineteen more between October 6 and 9, 1987. Blood samples were analyzed for hematology and serum chemical constituents including electrolytes, metabolites, enzymes, proteins and protein electrophoretic patterns, thyroid and adrenocortical hormones, and viral antibodies.

* Excerted from *Clinical Investigation of the 1987-88 Mass Mortality of Bottlenose Dolphins Along the U.S. Central and South Atlantic Coast* (final report to National Marine Fisheries Service and U.S. Navy, Office of Naval Research and Marine Mammal Commission, April, 1989) by J. R. Geraci, University of Guelph, Ontario, Canada

Results

Pathology

The study required numerous observers over a broad geographic area. Inconsistencies in reported findings were therefore inevitable. Despite the limitation, trends were noted in the condition of the stranded dolphins. Those that came ashore in August and early September 1987 had a range of skin lesions. Small blisters and pock-like craters were common over the head region, particularly around the lips and snout, and in the soft tissues of the mouth. The dorsal fin, flippers, and tail flukes were also affected to some extent. Rarely, the entire surface of the body was covered with round raised pox-like lesions measuring up to 1cm in diameter. Histologically, the lesions consisted of vacuolation and swelling of epidermal cell cytoplasm with no involvement of the dermis. A viral infection was suspected, and though inclusion-like structures were occasionally noted, they contained no convincing evidence of virus particles. Results of viral isolation from representative lesions are reported below (see Virology).

Other findings in the dolphins were also related to septicemia, and particularly to the effects on blood vessels which had been injured by bacteria. The vessel walls became fragile and necrotic, and were unable to contain blood. Plasma leaked into tissue spaces causing edema in many of the organs, and accumulation of massive quantities of blood-tinged fluid in the thoracic and abdominal cavities. Affected organs underwent necrosis as a combined effect of impaired circulation and bacterial toxins. In some cases, the animals appeared to have died during the acute phase of bacterial infection. Others, less severely affected, had a more protracted illness which terminated a pneumonia, cerebral hemorrhage, secondary invasion by fungal organisms, and vascular collapse or shock.

In liver there was thickening of the capsule and fibrosis of parenchyma especially around portal triads and under the capsule. Some of this fibrosis was associated with parasitic infestation but elsewhere the fibrosis was typical of post-necrotic scarring. In several animals dying late in the outbreak there was severe hepatic lipidosis, hepatocellular anisokaryosis and single-cell necrosis consistent with toxic hepatopathy.

In many dolphins, lymphoid follicles in spleen, lymph nodes, and intestine were depleted. The centers of the follicles were hyalinized, and lacked lymphocytes.

Bacteriology

A wide variety of bacteria was recovered from stranded dolphins. The organisms include members of the genera *Edwardsiella, Streptococcus, Vibrio, Pseudomonas, Klebsiella, Acinetobacter, Bacillus, Staphylococcus,* and others. There was no particular pattern to their distribution within an animal. Members of the *Vibrio* group predominated, representing 52% of the total isolates. All tests for *Chlamydia* were negative.

Virology

Tissue specimens and lesions from dolphins were evaluated for the presence of viruses by electron microscopy, immunofluorescence, and cytopathic effects in tissue culture. No virus particles were observed in direct examination by electron microscopy, nor were antigens detected to influenza A and B, parainfluenza 1 and 3, varicella-zoster virus, herpes simplex 1 and 2, and adenovirus. All samples were negative for bovine leukosis, bluetongue, contagious ecthyma, equine infectious anemia equine rhinopneumonitis, vesicular stomatitis, and ovine progressive pneumonia. There was no evidence of retrovirus infection.

Serology

Canine distemper virus-neutralization assays on serum from live-captured dolphins showed inhibition of virus in 6 of 13 samples. Titers greater than 1:2 suggest that CDV antibody was present. One dolphin had a titer of 1:128, two of 1:24, two of 1:12, and one of 1:6. There was no apparent bias in sex or age of the positive dolphins.

Biotoxins

Eight of 17 stranded dolphins collected during the event tested positive for the neurotoxin: two of six collected near Virginia Beach in July and August, 1987; three of five in the same area between September 18 and October 8, 1987; and three of the six along northern Florida in January and February, 1988. There was no apparent correlation between the concentration of the toxin and the chronology or location of stranding. No PbTx-2 was demonstrated in any other dolphin liver sample, including the three animals that died during capture in October, 1987.

Brevetoxin was found in the viscera but not in the flesh of menhaden taken from the stomach of one dolphin; no toxin was detected in weakfish also taken from the same animal, nor from the liver of that dolphin. Of the seven species of fresh-caught fish tested, only the viscera of menhaden landed on February 20 and 28, 1988, contained detectable brevetoxin, at levels representing 200µg per fish.

Toxicology – Organochlorines

Average concentrations of organochlorines in blubber were higher in immature than in mature females, and showed the opposite pattern in males. Statistically (Newman-Keuls ANOVA), the difference between mature males and females was significant for DDE and PCB ($p<0.01$), and t-nonachlor ($p<0.05$). The highest concentration of residues was in a mature male with 1.3% lipid in blubber; PCB was 6800 ppm, DDE 2000 ppm, and t-nonachlor 400 ppm. There was a significant correlation (linear regression p_0.001) of PCB with

DDE, PCB with t-nonachlor, and DDE with t-nonachlor in blubber of all animals. The blubber of captive dolphins had PCB levels comparable to those of the immature animals; DDE and t-nonachlor levels were comparable to those immature males. The blubber lipid of the other cetacean species had significantly lower PCB than the stranded dolphins; there was no consistent pattern for the other contaminants.

The concentrations of contaminants in liver lipids of *T.truncatus* had a pattern similar to that in blubber. Levels of DDE were lower in mature females than in immature ($p<0.05$) and mature males (p_0.01). The captive dolphins had higher DDE levels than the average for the stranded group as a whole. Mature females also had lower values for t-nonachlor than immature males ($p<0.05$). The male with the highest levels of organochlorines in blubber also had the highest concentrations in liver – 5200, 1300, and 200 ppm for PCB, DDC, and t-nonachlor, respectively. These data were omitted from statistical computations so as not to skew the population mean. In the stranded pilot whales, PCB concentrations were below detectable limits, and DDE and t-nonachlor were significantly lower than in all but the mature female dolphins. As in blubber there were significant correlations ($p<0.001$) among all three classes of compounds in all groups of animals.

Toxicology - Heavy Metals

Liver concentrations of heavy metals did not differ significantly among immature and mature, male and female dolphins. As in other species, mercury and selenium levels were highly correlated; all values for heavy metals were comparable to those reported for other odontocetes.[2,3,4]

Discussion

This has been the most extraordinary saga of cetacean disease on record. Between the time the first dolphin stranded in New Jersey in June 1987 and last on Florida's east coast eleven months later, over 740 animals died. The exact toll is not know, since almost certainly some animals were not recovered. However, it is estimated that 50% or more of the coastal migratory stock between Florida and New Jersey died during this period.[1] Without a guiding precedent to help uncover the cause, it was necessary for the investigation to sweep a broad range of disciplines before settling on the eventual path to the probable solution. The two most likely potential causes for an outbreak of this kind were considered to be infectious disease and poisoning. After weighing evidence from 18 months of field and laboratory analyses, we have concluded that brevetoxin, the neurotoxin produced by the dinoflagellate

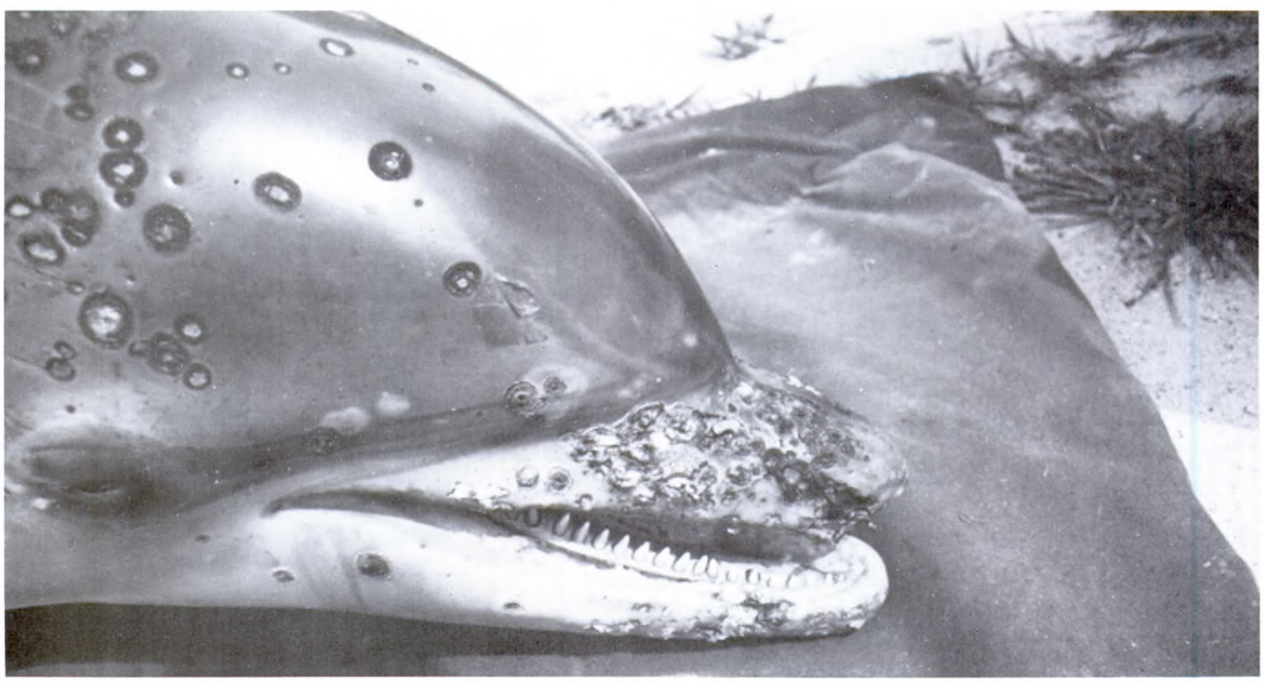

Figure 1

Generalized pox: Young dolphin with the pox-like skin condition which affected some of the stranded animals.

Ptychodiscus brevis, probably was the proximate cause of this devastating event.

Early findings led the investigators away from microbial agents as the principal cause of death. There was no single pattern of illness that could be associated with a known pathogen, though it was clear that infectious agents contributed to and sometimes dominated the clinical picture. The first animals to come ashore on Virginia Beach in late summer clearly had been ill for some time, with a condition that ultimately affected skin, liver, and lung, and led to the accumulation of fluid in the abdominal and thoracic cavities. Meanwhile, in New Jersey, Drs. W. Medway (University of Pennsylvania) and D. Roscoe (New Jersey Division of Fish, Game and Wildlife) indicated in personal communication that carcasses there were in better condition and less affected with secondary bacterial infection. It appeared these differences were regional; dolphins coming ashore on Virginia Beach died in warmer waters heavily contaminated with opportunistic bacteria. Over 50% of the 21 species of potentially pathogenic bacterial isolated from 48 dolphins were of the genus *Vibrio*. These seemed to have been associated with some of the problems in skin and blood vessels that ultimately killed many of the animals but were not the primary cause of disease. The overwhelming nature of some of the infections, which probably arose in the lung, may have been related to immunoincompetence, the cause of which cannot be established. The depletion of lymphoid follicles in spleen, lymph nodes, and the intestine supports this suggestion. (Figure 1)

Some dolphins also had viral infections. Eight had a skin condition characteristic of dolphin pox,[5] complete with suspicious inclusion bodies but in which no virus particles could be detected. In view of public sentiment expressed during the outbreak, it was comforting but not surprising to learn that none of the dolphins examined showed evidence of retroviruses, the group of viruses which is associated with Acquired Immune Deficiency Syndrome (AIDS) and whose counterparts in animals could have been a cause of reduced ability to fight normally harmless diseases. In any event, such viruses have a long latent period, and would not likely culminate in a single outbreak of disease. Dr. K. Somers is continuing to characterize the reovirus-like particles isolated from an ulcer on the palate of a dolphin[6]. It is premature to comment on the serological titers to canine distemper virus, a morbillivirus, in six of 13 blood samples. Kennedy *et al* have diagnosed morbillivirus infection and found distemper-like lesions in harbor porpoises (*Phocoena phocoena*) from the Irish Sea.[6] We found no evidence of such infection nor was a morbillivirus detected using techniques suitable for its propagation. It is possible that the dolphins had been previously infected with a virus that escaped detection, or was no longer present at the time of the outbreak. A study must be undertaken to determine whether the virus or other antigen responsible for the serological reaction is widespread in dolphins and whether it is a pathogen. This calls for an examination of blood samples from a broad range of cetaceans, and an investigation into the nature of the antigen.

Geographic and temporal patterns of mortality also lacked the hallmark of infectious disease. During August 1987, at least 125 dolphins stranded dead along the Virginia coastline; nearly 50 came ashore in each of the months before and after. Others, according to fish-spotter pilot Mr D. Thompson, were reported dead in small clusters at sea 18 miles from Cape May, NJ (August 21, 1987). To create such an overall pattern, an infectious agent would have had to be highly virulent — causing acute disease across all ages and both sexes, spreading rapidly over a broad geographic range, and killing groups of animals without pause. Viruses and some bacteria introduced either by airborne transmission or through direct contact are capable of producing such havoc. Seals exposed on crowded rookeries have fallen victim to epizootics of influenza,[7] morbillivirus,[8,9] and leptospirosis.[10] Yet, there is little to suggest that these or other contagious organisms could spread as explosively among cetaceans. Dolphins are more dispersed in an environment which, unlike air, solid substrate or even a closed body of water, would not readily support the transmission of such agents.

The accumulating evidence led us to consider a point source contaminant as the cause of mortality. This was also a subject of public concern, as reflected by a train of media reports that sewage and toxic wastes were being discharged in the New York Bight and Delaware Bay areas. We approached the Environmental Protection Agency to obtain information on permitted and illegal dumping of municipal and industrial wastes off the mid-Atlantic states, and submitted tissues for heavy metal and organochlorine contaminant analysis.

Levels of contaminants in the dolphins' blubber were found to be among the highest recorded for a cetacean.[11-15, 2] Unfortunately, it is not possible to compare the levels with those in other *T. truncatus* as the only study on this species employed a different technique.[16] To ensure that the high values were not an artefact of our methodology, we analyzed blubber and liver samples from pilot and humpback whales, and harbor porpoises, for which published data exist. Results of PCB, DDE, and t-nonachlor analyses on the pilot whales agree closely with the recent findings of Muir for the same species.[2] Residues in the blubber of humpback whales (DDE and PCB) are comparable to those reported by Taruski *et al*[17]. Our DDE and PCB values in the harbor porpoise are similar to or lower than reported by Gaskin's *et al*.[11,12] The values in *Tursiops* stand unreservedly among the highest in cetaceans - a commentary on the state of eastern coastal waters.

High organochlorine levels in *T. truncatus* were not restricted to the stranded group; the captives had concentrations similar to those in all but the stranded mature males. The results form the beach-cast specimens obviously reflect the levels of contaminants in the nearshore environment, where the dolphins accumulate these substances. The residues occur in the blubber of captives perhaps because they are given contaminated food, or more likely because with a steady diet, they have no need to mobilize blubber fat which would deliver the compounds to liver for excretion. Under these stable conditions, the presence of organochlorines in blubber may not pose a risk. Free-ranging animals facing intermittent food supply, or mobilizing fat during lactation, migration or times of illness, release compounds from this depot into vital, perhaps more critical organs such as liver.

Considering the evidence that at least some of the dolphins were mobilizing PCBs from blubber to liver, it is conceivable that blood levels rose and were sustained long enough to exert an effect. One class of organochlorines, the polychlorinated biphenyls (PCBs), can be harmful following both acute and chronic exposure. Typically affected are liver and skin, and nervous, reproductive, and immune systems.[18] Yet we cannot categorically relate any of the conditions observed in the dolphins to the known effects of these compounds because of vast differences in response within and between species. Furthermore, it is unlikely that contaminants were the key to the event. The timing of the outbreak would have required that these compounds be mobilized to functionally toxic levels within a synchronized time-pulse. This is an unlikely scenario for substances which for decades have been a constant ingredient in their environment and body tissues, unless something else triggered their release by first debilitating the dolphins.

Biotoxins were considered to have this capability. The possibility was strengthened when saxitoxin, a neurotoxin produced by marine dinoflagellates, was found to be responsible for the deaths of 14 humpback whales, *Meqaptera novaeanqliae,* in early December 1987 and January 1988, in Cape Cod Bay (Geraci *et al.* in press). On the heels of that study, we analyzed liver samples from 17 dolphins that had died during the early, middle and late phases of the outbreak. There was no evidence of saxitoxin in these tissues.

By late summer 1988, some of the dolphin liver samples were reported to contain brevetoxin (PbTx), a lipid-soluble polyether toxin produced by unarmored marine dinoflagellate Ptychodiscus brevis, Florida's red tide organism. The neurotoxin is extraordinarily potent, capable of generating effects in the nanomolar to picomolar concentration range *in vivo* (Baden, in press). When the analyses were completed in January, 1989, PbTx was found to be in the livers of eight of the 17 beached dolphins collected during the outbreak. No toxin was detected in any of the 17 controls, selected from dolphins that died in captivity, others in regions or at a time not related to the fatalities under investigation, and three that died during capture in October, 1987. A greater number of analyses would have added statistical weight to these findings. Yet the tests are time-consuming, and by this writing, 34 dolphins samples in addition to the fish specimens were all that could be processed. The pattern is nevertheless clear: 47% of the 17 diseased animals contained the toxin; all the rest did not.

Levels in dolphins liver ranged between 80-16,000 ng/g, and the calculated total amount in that organ was 0.08-14.7 mg. Assuming all the toxin was confined to liver, the total body burden would have been 2-290 g/kg, comparable to or orders of magnitude higher than the 2.85 g/kg level known to cause illness in man. [19] These values are conservative. Standard extraction procedures are only quantitative for one unaltered form of PbTx. Other forms that are covalently bound or otherwise modified were not considered. Nor is it reasonable to assume that all the toxin was in liver.

Signs of PbTx poisoning in fish and mammals are related to its action on the nervous system. Mice lose motor control, become paralyzed and die of respiratory arrest. [20] The site of action is the voltage-sensitive sodium channel in excitable membranes, where the toxin causes increased sodium flux with subsequent depolarization and persistent activation of excitable cells. [21] Death is rapid, and there are no reports of discernable histopathologic changes in acutely poisoned animals. Might this account for the presence of PbTx in a menhaden recently consumed by dolphin KDL-644 that showed no evidence of toxin in its liver? (Figure 2)

Most of the dolphins did not die this way. They manifested an array of chronic disorders including fibrosis of liver and lung, adhesions of abdominal and thoracic viscera, and secondary microbial infections associated with immune suppression, as evidenced by histological changes in lymph nodes. We suggest sublethal exposure to PbTx precipitated the train of events leading to some or all of these chronic changes. PbTx promotes peripheral vasodilation[20] and is cardiotoxic.[22] As a toxic aerosol, or once absorbed, it disrupts neural control or respiration[23] and induces bronchoconstriction.[24] Symptoms of poisoning in humans reflect the gastrointestinal and neurologic action of the toxin. They include nausea, vomiting, diarrhea, reversal of temperature sensation, ataxia, and numbness and tingling of extremities.[25] A dolphin so affected would likely stop eating, eventually exhaust its blubber reserve, and thereby lose its passive buoyancy and thermal shield. The stress associated with these changes alone could set the stage for infection by the ubiquitous opportunistic organisms that were isolated from the affected dolphins. Superimposed on this, any direct neurotoxic effect of PbTx would be particularly threatening to a diving mammal.

How were dolphins exposed to the toxin? Red tides in southeastern U.S waters normally originate 20-75 km west of the central Florida cost in the Gulf of Mexico, and generally remain within the Gulf where they eventually dissipate.[26] Occasionally, as in 1972, 1977, and 1980 they can be entrained and transported to the east coast of Florida by the Gulf Loop Current - Florida Current - Gulf Stream system.[27,28] This happened in the fall of 1987, and resulted in the eventual

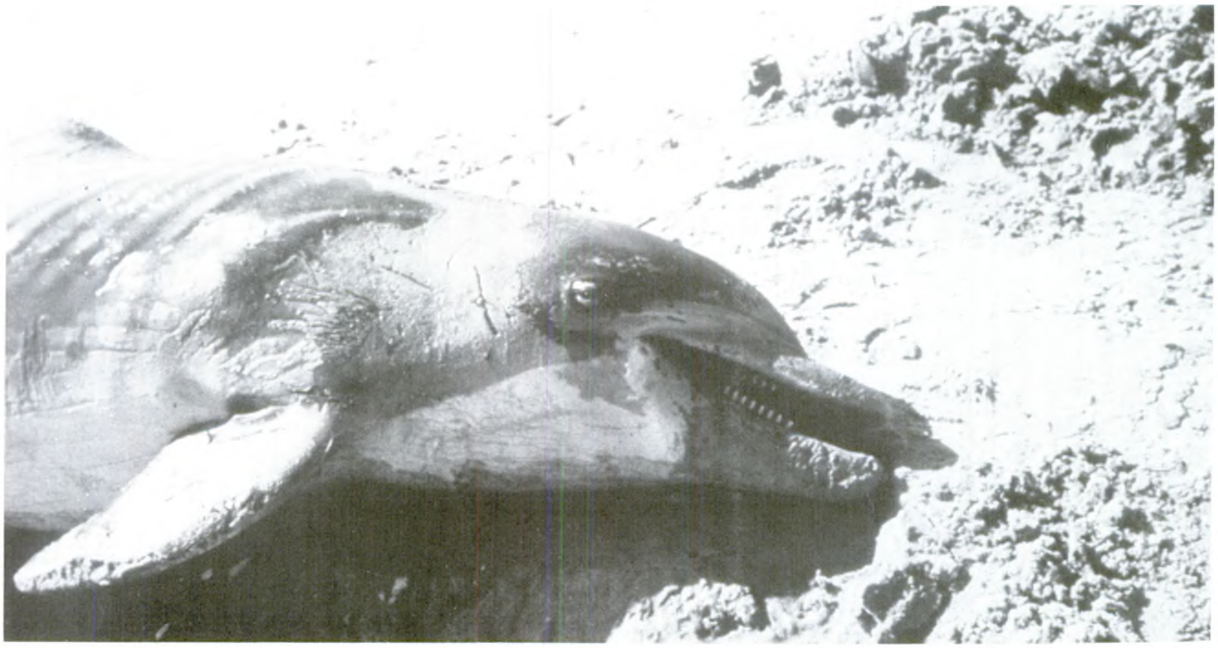

Figure 2

Emaciated dolphin that was cast ashore dead. Many of the affected animals showed evidence of fasting or starvation.

closure of shellfish beds along the North Carolina coast; there also were reports of respiratory and eye irritation in fishermen and residents.[29] Yet the toxin was found in the livers of dolphins that beached in Virginia three months before that time. They must have encountered the organisms sometime and somewhere along their northerly migration route.

In February, 1987, a *P. brevis* bloom was 25 km from a point where Gulf waters are transported to the east coast. Drift bottle data suggest that a fragment could have reached the east coast by spring of that year.[30] The possibility exists that blooms had been occurring all summer in and adjacent to the Gulf Stream, and went undetected until a filament reached the North Carolina coast in October, 1987. Such blooms would have been difficult to detect at sea, as they are not easily seen from vessels and there would have been little in the way of toxic aerosols, which are generally produced by waves and by surf action in shallow waters. Planktivorous fish might have consumed the cells offshore during their migration northward. And dolphins could have obtained the toxin by eating these fish or their predators. These conditions would have exposed dolphins both directly in water, and indirectly in food, to PbTx for an extended period, with effects manifested a short time later as they reached the mid-Atlantic coast.

Brevetoxin was recovered from three yellowfin menhaden, *B. smithii*, caught off Vero Beach, Florida, in late February 1988, and one unidentified menhaden taken from the stomach of a dolphin that stranded near Cape Canaveral on January 12, 1988. The finding of brevetoxin in fish at that time and place suggests that there was a persistent, undetected bloom that kept the food-web contaminated through the winter. Alternatively, the bloom that had delivered the filament to North Carolina in October 1987, had dissipated and left fish contaminated for at least three months. The first scenario challenges our understanding of the process of *P. brevis* blooms, the second of the dynamics of brevetoxin transfer in marine organisms.

In the fall of 1987, on their southerly migration, dolphins encountered the bloom off North Carolina. P. Tester (NOAA-NMFS Beaufort Laboratory, personal communication) observed dolphins surfacing in the blooms at that time. Three months later, and perhaps all along, they were feeding on contaminated fish. We believe that this second encounter with the toxin was responsible for the wave of stranded animals recovered along the Florida coast in the winter of 1987-1988; three of six dolphins examined had PbTx-2 in liver.

Levels of PbTx in the viscera of the live-caught menhaden translate to 200μg of toxin per 500 g fish. Using this value, a dolphin feeding on menhaden at a rate of 10 kg each day, would consume 4 mg of PbTx. That is below the 6 mg/kg LD50 for mice, but if general toxicological dogma is applied, much lower doses would be required to incapacitate an animal as large as a dolphin. In fact, only 0.2 mg can cause illness in people.

Not all the dolphins were poisoned by eating fish. PbTx was found in the livers of three nursing calves. Dolphin WAM 295, with the highest concentration of PbTx in liver, was estimated to be less than three months of age. The toxin had to have been delivered in the milk, suggesting that like other lipid soluble residues, PbTx may be stored in fatty depots and mobilized along with fats as the animal draws on these reserves. There is no precedent for the finding of PbTx in milk, nor has this route of PbTx elimination been considered.

The circumstantial evidence suggests that PbTx is the most probable cause of the mortality. Contributing to the ultimate demise of the animals was a host of microbial and environmental factors. This is unlikely to have been the first time that dolphins have been exposed to the toxin. *P. brevis* blooms regularly occur on the Gulf coast of Florida. There they are restricted geographically in contrast to dolphins which move about freely. The chance of encounters is therefore reduced. They do occur, and at least one other associated mortality of dolphins has been reported.[31] Because there has been no search for biotoxins in stranded animals, other poisoning would have gone undiagnosed. One might also speculate that dolphins in the Gulf of Mexico have encountered blooms often enough to associate malaise with the ingestion of toxin-containing organisms or the aerosol, and thereafter avoid contact.

The episode along the east coast obviously required that the circumstances that delivered the organisms there be coupled with the presence of carrier-fishes situated in the path of migrating dolphins. The unparalleled scope of this event would suggest that all of these conditions have been met rarely, if at all, in the past. The summer of 1987 was unusual by any measure. In North Carolina, human poisoning from consumption of fish[32] and shellfish[29] further attest to the unusual conditions that year.

The toxin in yellowfin menhaden has relevance to human health. Though not a fish that is commercially harvested, its southern range overlaps with related species of surface-feeding planktivores that are. In this case, the toxin was present in viscera and not the flesh, thus presenting no risk to humans consuming traditionally prepared fish, or the oils which are extracted under conditions that should destroy the toxin. [33]. To establish whether a risk in fact exists, studies should be directed toward determining the uptake, distribution, persistence and transfer of PbTx in some representative commercially exploited species.

The discovery of PbTx in the dolphins and its previous circumstantial link to manatee deaths lead to a new generation of thought on factors contributing to natural mortality of marine mammals.[34] Many questions will remain unanswered until directed studies are pursued. They must include: judicious examination of a representative sample of stranded marine mammals for biological toxins; studies on effects of chronic, sublethal exposure to PbTx; retrospective correlations between blooms and peak episodes of mortality; and determination of the environmental conditions that led to the unusual event of 1987. Equally important is the need to resolve the growing question of whether contaminants at levels found in the dolphins might have affected their resilience and rendered them more susceptible either to the toxin or to the microorganisms that eventually brought them to their demise.

Table 1

Analytical disposition of specimens collected during the 1987-1988 mass mortality of bottlenose dolphins.

ANALYSIS	NO. OF DOLPHINS	NO. OF ANALYSES
Complete necropsy	298	–
Histopathology	95	2,660
Bacteriology	48	117
– *Chlamydia*	42	116
Virology	63	721
Toxicology		
– Organochlorine	75	1,456
– Heavy metals	68	1,079
Biotoxins		
– Water soluble	13	13
– Lipid soluble	34	34
Clinical pathology	26	1,106

Biography

Dr. Joseph R. Geraci has been Professor, Department of Pathology, Ontario Veterinary College, University of Guelph, Ontario, Canada, for the last eleven years. From 1984 to 1986, he was visiting Professor, Tufts University School of Veterinary Medicine, Massachusetts. His research and publications in the field of marine mammals have been primarily concerned with: natural mortality, strandings, effects of environmental contaminants, pathophysiology, nutrition and health care.

References

1. Scott, G.P., D.M. Burn and L.J. Hansen. 1988. The dolphin dieoff: long-term efforts and recovery of the population. Proc. Oceans '88, Baltimore, MD. pp. 819-823

2. Muir, D.C.G., R. Wagemann, N.P. Grift, R.J. Norstrom, M. Simon and J. Lien. 1988. Organochlorine chemical and heavy metal contaminants in white-beaked dolphins *(Lagenorhynchus albirostris)* and pilot whales *(Globicephala melaena)* from the coast of Newfoundland, Canada. Arch. Environ. Contam. Toxicol. 17: 613-629.

3. O'Shea, T.J., R.L. Brownell, Jr., D.R. Clark, Jr., W.A. Walker, M.L. Gay, and T.G. Lamont. 1980. Organochlorine pollutants in small cetaceans from the Pacific and south Atlantic Oceans, November 1968 - June 1976. Pesticides Monitor. J. 14 (2): 35-46

4. Honda, K., R. Tatsukawa, K. Itano, N. Miyazaki and T. Fujiyama. 1983. Heavy metal concentrations in muscle, liver, and kidney tissue of striped dolphin, *Stenella coeruleoalba*, and their variations with body length, weight, age and sex. Agri. Biol. Chem. 47: 1219-1228

5. Geraci, J.R., B.D. Hicks,D.J. St. Aubin. 1979. Dolphin pox: a skin disease of cetaceans. Can. J. Comp. Med. 43 (4): 399-404

6. Kennedy, S., J.A. Smyth, P.F. Cush, S.J. McCullough, G.M. Allan and S. McQuaid. 1988. Viral distemper now found in porpoises. Nature 336:21

7. Geraci, J.R., D.J. St. Aubin, I.K. Barker, R.G. L-Webster, et al. 1982. Mass mortality of harbor seals; pneumonia associated with influenza A virus. Science 215: 1129-1131.

8. Mahy, B.W.J., T. Barrett, S. Evans, E.C. Anderson and C.J. Bostock. 1988. Characterization of a seal morbillivirus. Nature 336 (10):115

9. Octerhaus, A.D.M.E. and E.J. Vedder. 1988. Identification of virus causing recent seal deaths. Nature 335: 20.

10. Vedros, N.A., A.W. Smith, J. Schonwald, G. Migaki and R. Huddard. 1971. Leptospirosis epizootic among California sea lions. Science 172: 1250-1251.

11. Gaskin, D.E., M. Holdrient and R. Frank. 1971. Organochlorine pesticide residues in harbour porpoises from the Bay of Fundy region. Nature 233: 499-500

12. Gaskin, D.E., R. Frank, M. Holdrinet. 1983. Polychlorinated biphenyls in harbour porpoises, *Phocoena phocoena* (L), from the Bay of Fundy, Canada and adjacent waters, with some information on chlordane and hexachlorobenzene levels. Arch. Environ. Contam. Toxicol. 12: 211:219

13. Aguilar, A. 1983. Organochlorine pollution in sperm whales, *Physeter macrocephalus*, from the temperate waters of the Eastern North Atlantic. Mar. Pollution Bull. 14 (9): 349-352.

14. Tanabe, S., H. Tanaka and R. Tatsukawa. 1984. Polychlorobiphenys, EDDT, and hexachlorocyclohexane isomers in the western North Pacific ecosystem. Arch. Environ. Contam. Toxicol. 13: 731-738.

15. Martineau, D., P. Beland, C. Desjardins and A. Lagace. 1987. Levels of organochlorine chemicals in tissues of beluga whales (*Delphinapterus leucas*) from the St. Lawrence Estuary, Quebec, Canada. Arch. Environ. Contam. Toxicol. 16: 137-147.

16. King, C.A. 1987. Organochlorines in bottlenose dolphins (*Trusiops truncatus**) and pygmy sperm whales (*Kogia breviceps*) from southeastern Florida. M.Sc. Thesis. University of Miami. 92pp.

17. Taruscki; A.G., C.E. Olney and H.E. Winn. 1975. Chlorinated hydrocarbons on cetaceans. J. Fish. Res. Board Can. 32; 2205-2209.

18. Safe, S. 1985. Polychlorinated biphenyls (PCBs) and polybrominated biphenyls (PBB): biochemistry, toxicology and mechanism of action. Critical Reviews in Toxicol. 13: 319-395.

19. McFarren, E.F., H. Tanabe, F.J. Silva, W.B. Wilson, J.E. Campbell and K.J. Lewis. 1965. The occurrence of the ciguatera-like poison in oysters, clams, and *Gymnodinium breve* cultures. Toxicon 3: 111-123.

20. Baden, D.G. and T.J. Menda. 1982. Toxicity of two toxins from the Florida red tide dinoflagellate *Ptychodiscus brevis*. Toxicon 20: 457-462.

21. Poli, M.A., C.B. Templeton, J.G. Page and H.B. Hines. 1989. Detection, metabolism, and pathophysiology of the brevetoxins PbTx-2 and PbTx-3. In Natural Toxins from Aquatic and Marine Environments. S. Hall (ed.). Amer. Chem. Soc. Symp. Series, Washington, DC (in press).

22. Rodgers, R.L., H.N. Chou, K. Temma, T. Akera and Y. Shimizu. 1984. Positive inotropic and toxic effects of brevetoxin-B on rat and quinea pig heart. Toxicol. Appl Pharmacol. 76:296-305.

23. Borison, H.L., Ellis, S. and L.E. McCarthy. 1980. Central respiratory and circulatory effects of *Gymnodinium breve* toxin in anesthetized cats. Br. J. Pharmacol. 70: 249-256.

24. Baden, D.G. 1983. Marine food-borne dinoflagellate toxins. Int. Rev. Cytol. 82: 99-150.

25. Baden, D.G., T.J. Meade, G. Bikhazi and I. Leung. 1982. Bronchocon-striction caused by Florida red tide Toxins. Toxincon 20: 929-932.

26. Steidinger, K.A. and K. Haddad. 1981. Biologic and hydrographic aspects of red tides. Bioscience 31 (11): 814-819.

27. Roberts, B.S. 1979. Occurrence of *Gymnodinium breve* red tides along the west and east coasts of Florida during 1976 and 1977. In Toxic Dinoflagellate Blooms. D.L. Taylor and H.W. Salinger (ed.). Elsevier/North Holland, NY. pp. 199-202.

28. Steidinger, K.A. and D.G. Baden. 1984. Toxic marine dinoflagellates. pp. 201-261. In Dinoflagellates. D. Spector (ed.). Academic Press, NY.

29. Tester, P.A., P.K. Fowler and J.T. Turner. 1989. Gulf stream transport of the toxic red tide dinoflagellate, *Ptychodiscus brevis* from Florida to North Carolina. In Proc. Symp. on Novel Phytoplankton Blooms: Causes and Impacts of Recurrent Brown Tides and Other Unusual Blooms. Stony Brook, NY (in press).

30. Williams, J.W.F. Grey, E.B. Murphy and J.J. Crane. 1977. Drift bottle analyses of eastern Gulf of Mexico surface circulation. In Memoirs of the Hourglass Cruises. Vol. IV, Part III. Publ. by Mar. Res. Lab., FL Dept. Nat. Res., St. Petersburg, FL. 133 pp.

31. Gunter, G., R.H. Williams, C.C. Davis and F.G. Smith. 1948. Catastrophic mass mortalities of marine animals and coincident phytoplankton bloom on the west coast of Florida, November 1946 to August 1947. Ecol. Monogr. 18: 309-324.

32. Bonaventura, J. and C. Bonaventura. 1987. Carolina fish may be toxin carriers. Environs 10(3): 1. Duke Univ. Marine Laboratory, Beaufort, NC.

33. Poli, M.A. 1988. J. Assoc. Offic. Anal. Chem. 71: 1000-10002.

34. O'Shea, T.J. and G.B. Rathbun. 1983. Summary report on a die-off of the West Indian manatee (*Trichechus manatur*) in Lee County, Florida, Spring 1982. Unpublished Report. Sirenia Project, Denver Wildlife Research Center, Gainesville Field Station, Gainesville, FL.

Wavelet Analysis and Radar Scattering from Water Waves

by Larry F. Bliven and Bertrand Chapron, Goddard Space Flight Center
National Aeronautics and Space Administration

Introduction

Predicament: Classic Fourier transformation techniques depict entire data sets in the frequency domain and thus we can not tell when various events occur.

Solution: A new multi-scale analysis technique, wavelet transformation, generates time-frequency graphs from usual time series data. With this tool, we can see the timing of high frequency components relative to lower frequency scales!

Significance: Wavelet transformation theory is established on a firm mathematical basis that relates it to traditional sampling theory, and yet it provides a new way to investigate physical processes.

Applications: Wavelet analysis is applicable to a broad range of topics, such as sonar, electromagnetic propagation in the atmosphere, and image analysis.

We briefly describe the mathematical properties of wavelet transformations and identify some of the outstanding contributions to its formalization in the next section. Then, we present wavelet transform images for interpretation of scatterometer response from sea-surface geometry.

Wavelet Transform Fundamentals

Heuristic Development

The Fourier transform of a function can be expressed as:

$$f(t), -\infty < t < \infty ; \hat{f}(\omega) = \int_{-\infty}^{+\infty} dt\, e^{(-i\omega t)} f(t) \quad (1)$$

So, we get a measure for all frequencies. But time localization is lost, and we can not tell when special events occur.

As a initial attempt to localize Fourier Transform output, we can use a time window g(t) in the Fourier integral. At a time b and frequency ω, the Window Fourier transform is defined by:

$$G f(b, \omega) = \int_{-\infty}^{+\infty} dt\, e^{(-i\omega t)}\, g(t-b)\; f(t) \quad (2)$$

It measures locally, in the region of time b, the amplitude of the sinusoidal wave component of frequency ω. The window function g is real and the energy of its Fourier transform is concentrated in the low frequency band. A square window function is sometimes used as an initial form, and it has been used with definition (2) to develop the fast and simple differential-spectral-analysis technique.[1,2]

A problem arises with differential-spectral-analysis when the phenomenon of interest is broad-band. For example, we can easily observe short capillary waves on long gravity waves. Thus, the window size is imposed by the lowest frequency components and we still lose localization of high frequency components. We need to adapt the size of the window to match the feature scale, and so:

$$G f(b, \omega) = \int_{-\infty}^{+\infty} dt\, e^{-i\omega t}\, g(t-b; \omega)\, f(t) \tag{3}$$

For this simple development, if we use a square window, we must acknowledge the side lobe problem in the sinus-cardinal distribution. To improve smoothness, energy conservation and maximal concentration of the shape in time and Fourier space, we replace the square window by a Gaussian window. From an initial function $g(t ; \omega)$ we obtain a general set of functions for each different scale, as:

$$a > 0,\ g^{a}(t;\omega) = \frac{1}{\sqrt{a}}\, g\left(\frac{t}{a}; \omega\right) \tag{4}$$

$$g^{a}(t;\omega) = \sqrt{a}\,\hat{g}(t ; a\,\omega) \tag{5}$$

The window functions $g^{a}(t ; \omega)$ have the same shape as $g(t ; \omega)$, but the duration is controlled by the scale parameter a; i.e., a > 1 corresponds to contraction (high frequency), and a < 1 is dilation (low frequency). So the frequency domain is determined by both the frequency ω (commonly chosen to be the Fourier spectral peak frequency) and the variation of parameter a (from the set of strictly positive real numbers). The definition (3) becomes:

$$a > 0,\ -\infty < b < \infty;\ W f(b, a) = \int_{-\infty}^{+\infty} dt\, \psi^{*(b,a)}(t)\, f(t) \tag{6}$$

The * denotes the conjugate complex, with

$$\psi^{(b,a)}(t) = \frac{1}{\sqrt{a}}\, \psi\left(\frac{(t-b)}{a}\right) \tag{7}$$

and

$$\psi(t) = e^{+i\omega t}\, e^{-\frac{t^2}{2}} \tag{8}$$

Thus the function f is measured in the sense of an inner product, as given in equation (6), on the space described by the set of dilated and shifted, unique analyzing functions ψ.

Rigorous Development

Recent advances in theoretical mathematics provide the means to generalize and assimilate concepts presented in the previous section into established mathematical theory. Grossman and Morlet[3], Meyer[4], Daubechies[5,6], and others have pioneered wavelet transformation theory by employing rigorous mathematical formulation to establish it as a super-set of sampling theory. We present a short review of the conditions that wavelet functions must fulfill and then examples of two common wavelet functions.

Any finite energy function f can be expressed by wavelet components $\psi^{(b,a)}$, (with wavelet coefficients Wf(b,a)), given in equation (6), if the wavelet ψ satisfies the following two conditions.

C1: finite energy condition,

$$\int_{-\infty}^{+\infty} dt\, \psi(t)^2 < \infty \tag{9}$$

C2: admissibility condition,

$$C_\psi = \int_{o}^{+\infty} \int_{-\infty}^{+\infty} \frac{d\,a\,d\,b}{a^2} |W\psi(b, a)|^2 = \int_{-\infty}^{+\infty} d\,\omega\, \frac{|\hat{\psi}(\omega)|^2}{\omega} < \infty \tag{10}$$

C2 implies ψ is bounded in time and frequency, and its Fourier transform $\hat{\psi}$ vanishes quickly to 0 in the neighborhood of ω=0, with $\hat{\psi}(0)$=0. So the analyzing wavelet has at least one oscillation.

When C1 and C2 are valid, equation (5) defines the wavelet transform as an isometry, (up to the constant $C\psi$), from the time space into the time-frequency map. The following general properties apply:

P1: energy conservation,

$$\int_{o}^{+\infty} \int_{-\infty}^{+\infty} \frac{d\,a\,d\,b}{a^2} |W f(b, a)|^2 = C_\psi \int_{-\infty}^{+\infty} dt\, |f(t)|^2 \tag{11}$$

P2: inversion formula,

$$f(t) = \frac{1}{C_\psi} \int_{o}^{+\infty} \int_{-\infty}^{+\infty} \frac{dadb}{a^2}\, W f(b, a)\, \psi^{(b,a)}(t) \tag{12}$$

P3: reproducing kernel,

$$W f(b'; a') = \int_{o}^{+\infty} \int_{-\infty}^{+\infty} \frac{dadb}{a^2}\, W f(b, a).$$

$$W f(b, a)\, K(b, b'; a, a') \tag{13}$$

Where the kernel K is

$$K(b, b'; a, a') = \frac{1}{C_\psi} \int_{-\infty}^{+\infty} dt\, \psi^{*(b,a)}(t)\, \psi^{(b',a')}(t) \quad (14)$$

P3 expresses the redundancy of the wavelet transform. Thus the wavelet transform is entirely determined by its values on a suitable grid (b,a), and we can extend all the continuous definitions to the discrete domain.

Wavelet Examples

For our needs, to describe as precisely as possible a wind-wave field, we chose two appropriate wavelets.

The first is used to quantify the relatively smooth surface-elevation time-series. It is a wavelet that looks like a 'modulated Gaussian', (Figure 1a), and it is defined as:

$$\psi(t) = (e^{(-i\omega t)} - C)\, e^{-\frac{t^2}{2}} \quad (15)$$

with

$$C = e^{-\frac{\omega^2}{2}} \quad (16)$$

This wavelet was initially advanced by Morlet[7], who proposed $\omega = \pi\sqrt{2/\ln 2}$ to make the correction term negligible (constant C in definition 15). The Gaussian envelope of the Morlet wavelet achieves optimum resolution in time and frequency spaces as shown by the Heisenberg uncertainty theorem. With the Morlet choice, the wavelet is almost periodic and regular, and it reminds us of the fundamental shape of smooth waves. Some recent investigations to describe propagation of nonlinear deep-water wave packets have demonstrated the utility of this wavelet transform.[8]

To localize intermittent events, such as jumps or abrupt changes, other wavelets are more effective. Detection of events which change the sign of the second derivative of the function f can be achieved by using appropriate analyzing wavelets (second derivative of smoothing functions) because the events correspond to zero-crossings in the wavelet-coefficient time-series. The second derivative of the Gaussian, often referred to as the ' mexican- hat', (Figure 1b), is a common choice. It is:

$$\psi(t) = (t^2 - 1)\, e^{-\frac{t^2}{2}} \quad (17)$$

This wavelet can be the basis of analysis for non-explicit stationary periodic signals, such as wave slope records.

Experiments

We conducted experiments in the 20x1x1.5 m wind-wave tank at NASA Wallops. Wind-waves were generated by recirculating air, and regular waves were generated by a paddle operated at 2 Hz. Sensors were located at 8 m fetch. We estimated wind friction-velocities from wind speed profiles. Surface elevation was measured by 3 capacitance probes with 5 mm separation in an L-configuration. We computed surface slope from elevation gage data. We operated a 36 GHz radar system[9] at 30 degrees from nadir and pointing upwind. The 12x10 cm radar footprint was centered at the location of the capacitance probes. The capacitance probes modified the gain of the radar response, but radar time series were similar for cases in which the capacitance probes were in and out of the footprint. Because we are only interested in the shape of the radar time series and not the absolute magnitude, enhancement by the capacitance probes is not a major concern. Analog signals from all the sensors were simultaneously digitized at 100 Hz for a total of 2k samples each.

Figure 1

Wavelet Examples: (a) Morlet Gaussian wavelet, useful for analysis of smoothly varying signals; (b) 'Mexican hat' wavelet, useful for analysis of abruptly changing signals.

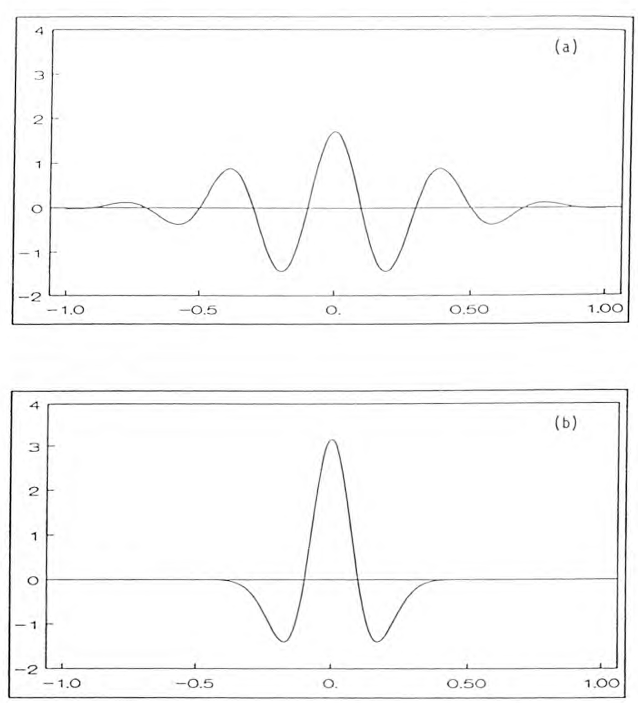

Results

We discuss two cases: (1) regular, low-level paddle-waves; and (2) mixed high wind-waves (u* = 82 cm/s) plus high paddle-waves. First we describe conditions in terms of traditional time series, then we present an introduction to interpreting time-frequency images. Lastly, we relate wavelet image features to the radar response.

Traditional Time Series

Elevation, slope, and radar time series are displayed for both cases in Figures 2 and 3. Let's review case 1. The periodic response at 2 Hz is due to the paddle-generated wave. As expected, a phase-delay of 90 degrees occurs between elevation and slope data; ie, maximum slope occurs on the front-face of the wave-crests. Because wave steepness is small (ak=0.08), there is little evidence of wave groups. The radar footprint is about a quarter of the paddle-generated wavelength, so the radar response varies as a function of long-wave phase. Thus, we see that for these regular waves, radar cross-section is periodic and highly correlated with long-wave slope. Radar cross-section has essentially uniform maxima occurring at 0.5 s intervals. We can observe that the radar maxima occur on the front-side of the wave crests which is when the surface is tilted towards the radar system.

Case 2 data are shown in Figure 3. Note that the vertical scales have been increased by a factor of 10 compared to Figure 2. Slope and elevation time series again exhibit the periodic response of the 2 Hz paddle-wave frequency. But for these conditions, the wave steepness is large, so the wave elevation and slope-time series are distinctly amplitude modulated, as shown by wave groups. Higher frequency wind-waves are present and can most clearly be seen in the irregular slope data and thus depict the variability due to different frequency components. The radar maxima are also highly variable and do not appear to be related to any single elevation or slope frequency component. The simple correlation between long-wave slope and radar cross-section observed for case 1 is gone. In nature, wind-wave spectra typically contain waves with frequencies that vary over several decades. Thus, we see the need for multiple-scale analysis in the time domain to characterize the radar return!

Figure 2

Paddle Generated Waves, Case 1.

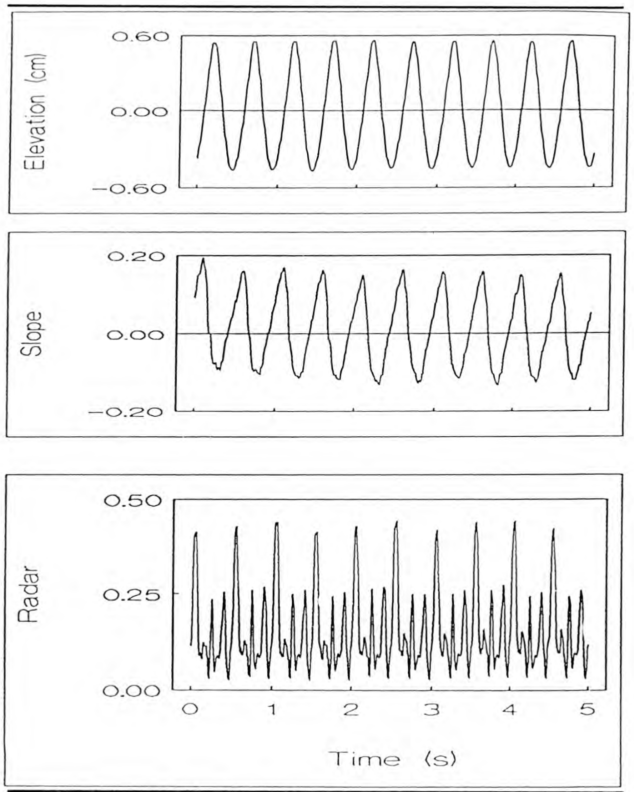

Figure 3

High -Wind plus Paddle Generated Waves, Case 2.

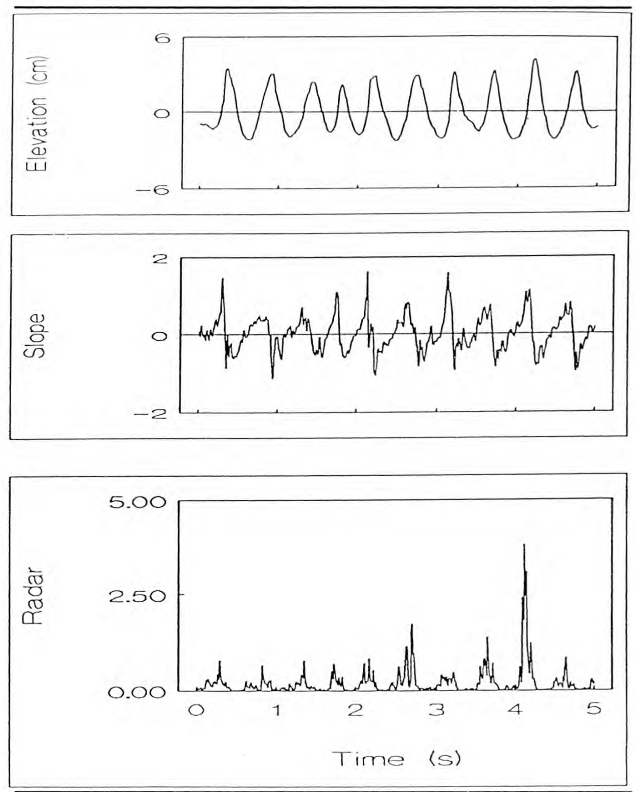

Wavelet Frequency-Time Images

We present time-frequency images of surface elevation and slope for cases 1 and 2, in Figure 4. Utilizing wavelet transform analysis, these images represent waterfall-displays of power-spectral-density (psd) versus time. Psd is defined in terms of the modulus of the wavelet coefficients given by Equation 6. In these images, the horizontal axis represents time, and the vertical axis ranges from 1 to 10 Hz (presented in a dyadic logarithmic format with 16 'voices' per octave). Psd magnitude is represented by 24 gray level coding. Elevation and slope wavelet images were constructed using Morlet and Mexican hat wavelets respectively. Data in each image were normalized by dividing by the maximum value. Finally, the integral of psd, for all frequencies at a particular time increment (vertical section), is proportional to the wave energy (variance) at each particular instant.

Let's examine case 1, paddle-generated wave images first. The dominant feature of the elevation image is a series of peaks at 0.25 s intervals due to the 2 Hz paddle-generated waves. Note, that with the time domain format, there is a psd maximum for each crest and trough. Although it may be difficult to see, there also is a second series of periodic peaks (at 0.125 s intervals) for the 4 Hz wavelets. These are the dominant wavelet's first harmonic and are traditionally represented by a Stokes-wave representation (primary plus harmonics, sinusoidal components). The image further reveals that total variance of wave crests is greater than that for troughs. Indeed, from the elevation time series, we measured the average crest and trough amplitudes to be 0.56 and 0.45 cm respectively. No organized pattern emerges for frequency components greater than 4 Hz.

Now let's review the slope wavelet image for case 1. First, for the 2 Hz dominant paddle-generated waves, the elevation and slope images show the 90 degree phase delay which was observed in the simple time series presentation (Figure 2). Slope images have maxima corresponding to the nodal points of the elevation time series. Notice the sharp decrease in total variance (vertical stripping, prominent at crests) corresponding to the peakedness of the 2 Hz slope component. See that the crest fronts are steeper, due to higher total variance of both 2 Hz and higher components, than the crest backs.

Elevation and wavelet images for case 2, high-wind plus paddle-generate waves, are also shown in Figure 4. The elevation image still shows psd peaks for the 2 Hz paddle-generated waves, but note the large amplitude variability of these components that is associated with wave groups. Higher frequency wavelets are enhanced due to the wind-wave generation. Also notice the large asymmetry of higher frequency components with respect to the dominant 2 Hz waves, revealing that crest fronts and backs are very different.

So what does this short data set suggest about radar power level relative to sea-surface geometry? Recall that the radar was pointing up-wind at 30 degrees from nadir. The strongest radar return corresponds to the front side of the long wave crest, near the nodal point, where the water surface is tilted toward the radar. The trough to crest nodal-points of surface elevation correspond to maxima in the slope time series. For paddle-generated waves, the radar response is coherent with the long wave slope. The radar response is more complicated when high wind blows over steep long-waves because the radar response is a function of multiple length scales on the water surface. Long-wave amplitude modulation contributes to variations in the radar response. But variability of the small-scale features such as short wind-generated waves and roughness associated with long-wave breaking also contributes to radar scattering characteristics. Assessment of the relative importance of these mechanisms to scatterometer response is beyond the scope of this paper, but we anticipate that wavelet transform techniques will provide a useful tool in this endeavor.

Figure 4

Wavelet Transform Images: Waterfall displays of power spectral density versus time.

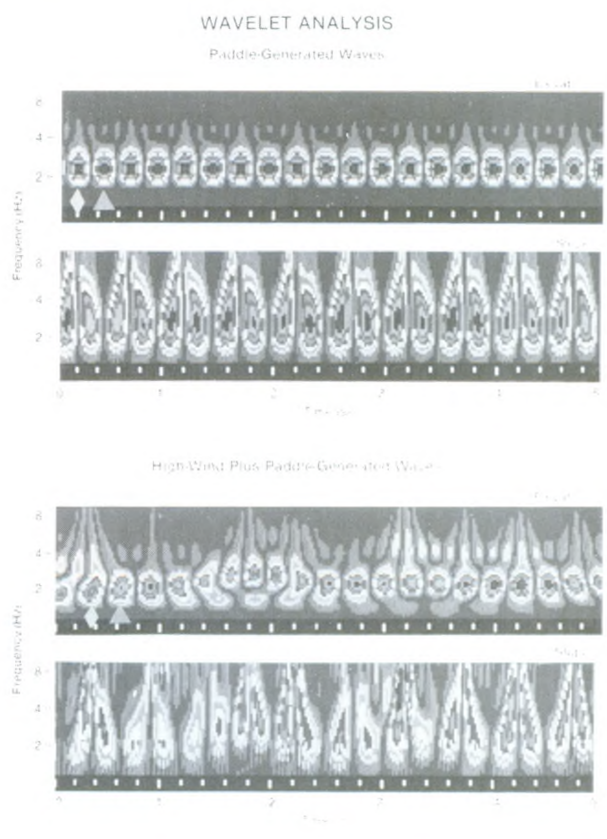

Summary

Wavelet analysis is an exciting new mathematical technique that provides multiple-scale information in the time domain. Its application potential is broad for both theoretical and practical applications: measure of fractal objects[10]; extensions to higher dimensions[11,12]; and data compression in technological design.

In the future, we plan to employ wavelet analysis to evaluate further and to formulate sea-surface microwave scattering models. We intend to extend wavelet computations to two dimensions in order to characterize slope and elevation images of the water surface with respect to short Bragg wavelengths being tilted by long waves.

Biographies

Larry F. Bliven, studies air-sea interactions, primarily on the micro-scale (centimeter scale). He received his Ph.D. degree at North Carolina State University in 1977. In 1985, he joined NASA and subsequently initiated work with Mr. G. Norcross of Computer Sciences Co. to develop microwave systems to study air-sea interaction processes in laboratory wind-wave tanks. He is presently investigating (a) rain effects on sea surface geometry as related to remote sensing, (b) microwave remote sensing as a tool for measuring air-sea gas exchange rates, and (c) new techniques for modelling microwave response to sea surface conditions. These activities are being pursued in cooperation with Drs. J.-P. Giovanangeli and A. Ramamonjiarisoa at the Institut de Mecanique et Statistique de la Turbulence (IMST), Marseille, Fr, and Dr. R. Wanninkhof at Lamont-Doherty Geological Observatory. His research is supported by NASA and ONR.

Bertrand Chapron, a French native, received his Ph.D. degree in fluid mechanics from the University II of Aix-Marseille, in 1988. Collaborating with Dr. A. Ramamonjiarisoa at IMST, he developed original numerical methods to investigate nonstationary data records. He presently is working as an NRC/RRA associate at NASA. In cooperation with the investigators at Wallops Island and Marseille, he is developing new techniques to describe experimental wave fields, and to interpret the different dynamical transitions in surface-waves. His primary research activities include extensions of wavelet transform techniques for multidimensional analysis are in progress and will be applied to remote sensing applications.

References

1. Gibiat, Jardin and Wu 1987. Acustica, vol 63.Conf. on Ocean-Atmosphere Interaction, AMS.

2. Bourguel, M. and B. Chapron, 1988. Methodes classiques et parametriques d'analyse spectrale, description et mise en oeuvre. Proceedings of the first International Conference in Africa on Computer Methods and Water Resources. Computational Mechanics Series. Springer Verlag.

3. Grossman, A. and J. Morlet. 1984. Decomposition of Hardy functions into square integrable wavelets of constant shape. SIAM J. Math., vol 15, pp 723-736.

4. Meyer, Y. 1986. Seminaire Bourbaki 1985/1986, no 662.

5. Daubechies, I., A. Grossman and Y. Meyer. 1986. Painless nonorthogonal expansions. J. Math. Phys., vol. 27, no. 5, pp 1271-283.

6. Daubechies, I. 1988. Time-frequency localization operators: a geometric phase space approach. IEEE Information Theory, vol. 34, no.4, pp 605-612.

7. Morlet, J., G. Arehs, I. Fourgeau and D. Giard, 1982. Wave propagation and sampling theory, Geophysics, vol 47, pp 203-236.

8. Chapron, B. and A. Ramamonjiarisoa. 1989. Analyses temps-frequences de la propagation d'ondes de surface non lineaires. Colloque GRETSI.

9. Bliven, L., J.-P. Giovanangeli, and G. Norcross, 1988. A study of rain effects on radar scattering from water waves. Seventh 10Holschneider, M. 1988. On the wavelet transformation of fractal objects. J. of Statistical Physics, vol. 50, no.5/6, pp 963-993.

10. Holschneider, M., 1988. On the wavelet transformation of fractal objects. J. of Statistical Physics, vol. 50, No. 5/6, pp 963-993.

11. Mallat, S. 1989. A theory for multiresolution signal decomposition: the wavelet representation. To appear in IEEE trans. on pattern analysis and Machine Intelligence, Tech. Rep. MS.CIS.87-22, U. of Penn.

12. Murenzi, R. 1988. Wavelet transforms associated to the N-dimensional euclidian group with dilatations: signals in more than one dimension. Institut de physique theorique,universite catholique de Louvain, B-1348, Louvain-la neuve, Belgium.

Profile in Science

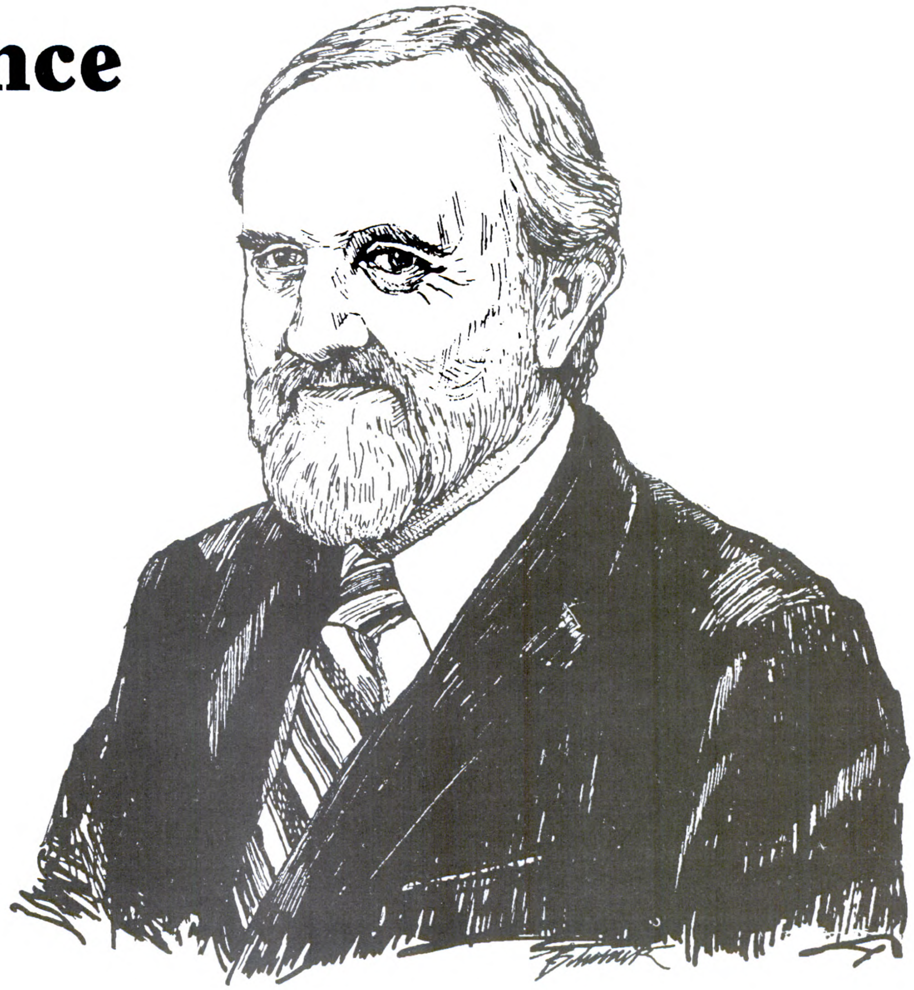

Dr. L. Eric Cross is Director of the Materials Research Laboratory and Evan Pugh Professor of Electrical Engineering at the Pennsylvania State University. He is an internationally recognized authority in the field of ferroelectricty. Ferroelectrics form the materials base for a wide range of capacitors, sensors, tranducers, actuators, and active composites. His recent studies have focused upon electromechanical tranducers. The results of these and other studies have been presented at many international and national conferences and are documented in more than 270 technical papers.

A native of England, Professor Cross attended Leeds University, earning his B.S. and Ph.D. degrees in Ferroelectricity. After a short period of work at the Electrical Research Association in England, Dr. Cross came to the Pensylvania State University in 1961, and became a founder of the Materials Research Laboratory. Dr. Cross was co-chairman for the first U.S. and China Seminar on Ceramics in 1983, and chaired the seminar in 1987. He was the U.S. chairman of both the first and second U.S. and Japan meetings on dielectric and piezoelectric ceramics. In April 1987, Dr. Cross was awarded the first honorary degree from Xian University in The People's Republic of China.

The New High-T_c Copper Oxide Superconductors:

On the Description of Their Normal State Properties

by Warren E. Pickett, Naval Research Laboratory

Introduction

The discovery of the new class of copper oxide superconductors which have transition temperatures T_c up to 100 K has provided a stunning turnabout in a field which has been characterized by small, methodical advances. For those of us who have devoted effort to the increase of T_c by a degree or two (or, in our maddest moments, five) the new developments still at times seem a dream almost beyond imagination. They are providing us with the moment of a scientific lifetime, and the possibility to make lasting contributions in an area of high excitement and, also, visibility.

Since the breakthrough by Bednorz and Müller[1] in the La-Ba-Cu-O system and the subsequent discovery by Chu and collaborators[2] and others in the Y-Ba-Cu-O system, the field has been deluged with scientific publications, press releases and hastily organized symposia at a wide variety of conferences dealing with condensed matter physics. Without any attempt to be exhaustive, I give the following list of meetings held during the first eight months of 1987 which included substantial symposia dedicated to the new high-T_c materials:

American Physical Society March Meeting, New York, March
European Physical Society Meeting, March
Materials Research Society Meeting, Anaheim, April
Novel Mechanisms of Superconductivity, Berkeley, June
NATO Summer School, Trieste, July
18th Intl. Conf. on Low Temp. Physics, Kyoto, August
Yamada Conf. XVIII on Superconductivity in Highly Correlated Systems, Sendai, August

Although the intense experimental effort ranges from the investigation of basic scientific questions to the development of commercial devices for application, the theoretical emphasis has been heavily weighted strictly toward the identification (or "prediction") of the mechanism behind the occurrence of superconductivity at such very high temperatures. The theoretical speculation has been encouraged by conference organizers and by the theoretical community itself, perhaps to the detriment of the early development of programs dedicated to investigate the wide variety of normal state properties which almost certainly must be understood before the superconductivity questions can be settled. A parallel can be drawn from the BCS[3] breakthrough — it drew on the investigations covering several decades into the normal state as well as superconducting state properties to build a successful theory of phonon-mediated superconductivity.

These new copper oxide materials display a wide range of behavior which lies somewhat beyond the experience of most theoreticians. (This is also true of the experimental arena, where ceramists and "metallicists" have endured a more macroscopic form of pairing interaction to carry out the preparation, characterization and study of samples.) The key to their behavior may lie in the mixed ionic-metallic character which is displayed by these compounds and which is rather foreign to most theoreticians, who tend for simplicity to class materials into metals, covalent semiconductors and ionic insulators. Indeed it is this mixed character which led Bednorz and Müller to investigate the copper oxides: they should possess a very strong electron-phonon interaction, perhaps bordering on the polaronic type seen in transition metal oxides, while retaining the metallic conductivity they expected to be necessary for a high T_c material.

At the Naval Research Laboratory (NRL) we have initiated, and indeed made considerable progress in, a theoretical program to develop a *quantitative understanding of the properties of copper oxide materials*, with initial emphasis on establishing the theoretical language which is necessary to describe the normal state properties. In addition to establishing the general electronic structure and the character of the bonding, important questions center on:

a. the effects of alloying (La with Ba or Sr, oxygen with vacancies),

b. the strength and characteristics of the electron-phonon interaction,

c. the correct description of the d.c. transport properties as well as the infrared and optical conductivity, and

d. the calculation and understanding of the lattice statics (including structural instabilities) and the lattice dynamics.

Any one of these properties, as well as some other possible ones, may be intimately related to the mechanism responsible for the high temperature superconductivity, but these relationships will not be emphasized here.

This report reviews the work done at NRL with the support of the Office of Naval Research during 1987. The group currently working on the high Tc materials consists of (in alphabetical order) Larry L. Boyer, Ronald E. Cohen, Barry M. Klein, Dimitri A. Papaconstantopoulos and myself at NRL and, in no less central roles, Henry Krakauer (College of William and Mary) and Philip B. Allen (SUNY/Stony Brook). A central point, which will be emphasized below, concerns the best approach to use to describe and to understand the properties of these unusual cuprates. It seems likely that they lie somewhere near a "Mott instability," a concept which arises

Figure 1

Crystal structure of the 2-1-4 class of compounds, with a blowup of the CuO_6 octahedron showing the interatomic distances.

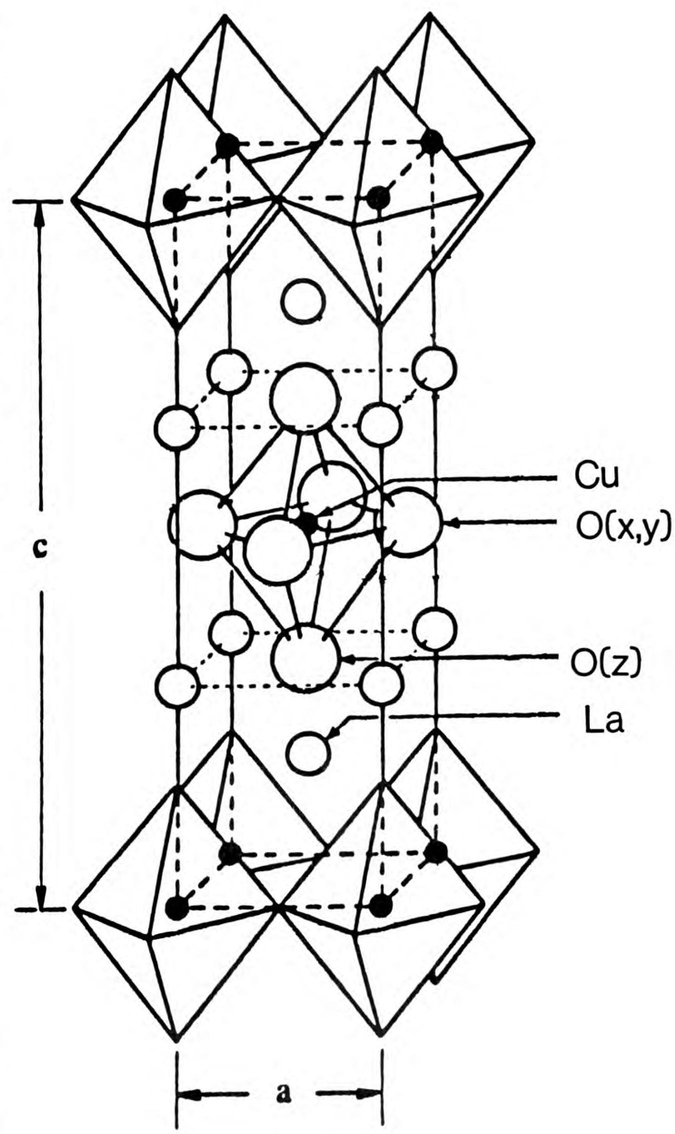

in the treatment of simplified model Hamiltonians (such as the Hubbard model) but which is not exactly definable for real materials. Brandow[4] has suggested the definition of a Mott insulator as a magnetic insulator which retains its local moment and insulating behavior above the magnetic ordering temperature. One may expect that in a Mott insulator the local density band structure gives a *qualitatively incorrect* picture of the single particle excitation spectrum. (The local density band structure never is more than an approximation to the quasiparticle spectrum, but often it is not only qualitatively correct but quantitatively quite accurate.) Typically this shows up as an insulating system which the local density approximation (LDA) predicts to be metallic.

Nomenclature: Bednorz and Müller, who have since been awarded the London Prize in low temperature physics and the Nobel Prize in physics for their efforts, discovered superconductivity in the La-Ba-Cu-O system near 30 K. This system, sometimes referred to as "Zurich oxide" after the place of discovery, has been established as occurring in a 2-1-4 composition as described below, and the "2-1-4" designation is common and will be used below. The class with T_c in the 90 K range will be referred to as the "1-2-3" system, which follows from the ratio of the metal atoms as discussed below.

Figure 2

Two views of the crystal structure of the 1-2-3 class of compounds.

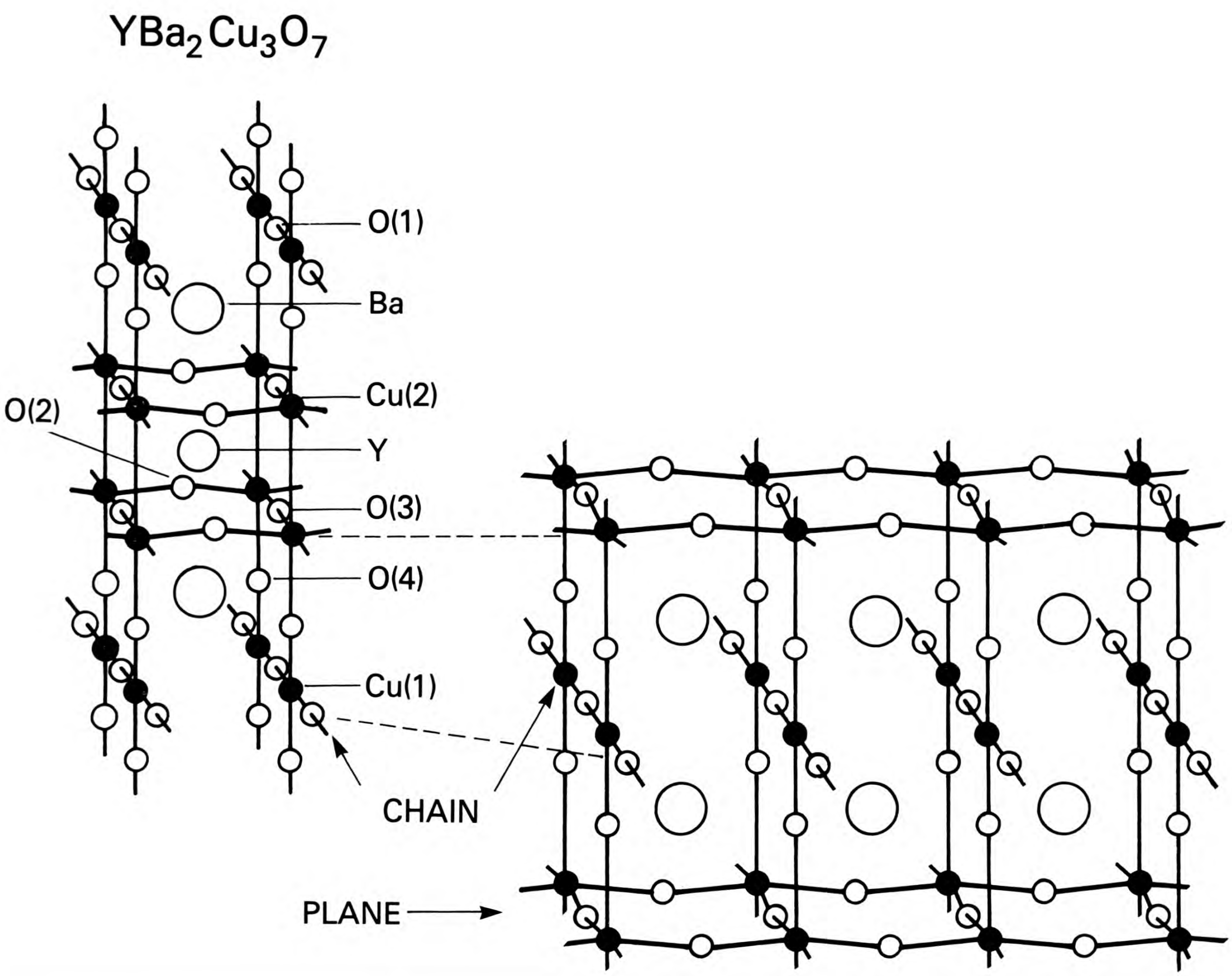

Average Crystal Structure

The class of cuprates with T_c in the 30-40 K range have the chemical formula $La_{2-x}M_xCuO_{4-y}$, where M is either Ba or Sr and the concentration y of O vacancies is usually greater than zero and may tend to increase with increasing x. The underlying structure[5], shown in Figure 1, consists of distorted CuO_6 octahedra which form a perovskite-like layer, and a layer of rocksalt-like La and O ions. The space group is body-centered tetragonal I4/mmm and the primitive cell contains one formula unit. The oxygens lie on two distinct sites, the in-plane $O_{x,y}$ and the out-of-plane O_z site, with the out-of-plane Cu-O distance being considerably larger (28%) than the in-plane Cu-O distance. The distortion of the Cu-O octahedron is generally described by physical chemists as due to a Jahn-Teller instability involving the d^9 shell of the Cu2+ ion.

For small O vacancy concentrations y less than or of the order of 0.05, which is the only regime discussed here, the pure La 2-1-4 compound distorts[6] to a lower symmetry orthorhombic structure (space group Abma) around T_s=500 K (decreasing with increasing x). This structural transformation now appears to be of the classic soft mode type[7], in which a soft (110) zone boundary "tilt" mode freezes into the lattice and results in the doubling of the primitive cell. The orthorhombic crystal structure has unequal in-plane lattice constants, and the two Cu-O octahedrons tip toward each other along the tetrahedral <110> direction by roughly 5 degrees. There are reports of transformations to lower symmetry structures being detected at low temperature.

Below the structural transition temperature La_2CuO_{4-y} becomes antiferromagnetic (AFM) at T_N around 240 K or below[8]. The AFM state is extremely sensitive to the O vacancy concentration, for if y is very much larger than 0.03 T_N is severely depressed or even driven to zero. The ordered moment appears to be no more than 0.5 Bohr magnetons per unit cell and is associated primarily with the Cu ion. Since the moment seems to be much lower in some samples, the AFM order could be interpreted more as the itinerant spin-density-wave type than a local-moment type, in spite of its commensurate nature. Recent experiments on single crystal samples reveal that long range coherent magnetic fluctuations remain well above the ordering temperature[9], which favors a local moment picture.

The high T_c 1-2-3 compounds typified by $YBa_2Cu_3O_{7-y}$ crystallize in a defect-perovskite structure[10], characterized by a superlattice ordering of the trivalent (Y) and two divalent (Ba) ions along one of the coordinate axes. This ordering is accompanied by a complete lack of oxygens in the plane of Y ions, as well as lacking 1+y oxygen atoms in the Cu-O plane between the Ba planes. At high temperature the O vacancies in this plane are randomly placed on the two sites and the space group is tetragonal P4/mmm. If the material is cooled slowly, an order-disorder transition occurs in which essentially all of the O vacancies take up one of the two sites. The resulting space group is orthorhombic Pmmm.

The resulting crystal structure is shown in Figure 2. Cu and O atoms form chains (or "ribbons") along one of the in-plane directions, taken here as the orthorhombic *b* axis. Due to the ordering *b* becomes somewhat larger than the other in-plane lattice constant *a*. Actual crystals of this material are usually highly twinned, which is expected to result from the different nucleation sites in the ordering process. In the ordered structure the chain Cu1 atom is 4-fold coordinated by O atoms in a distorted square-planar arrangement, while the

Figure 3

Thermal ellipsoids of La_2CuO_4 in the tetragonal structure, from Ref. 11. In the tetragonal phase the La (Ba) atoms have associated ellipsoids (not shown in the figure) similar to the out-of-plane oxygen atoms.

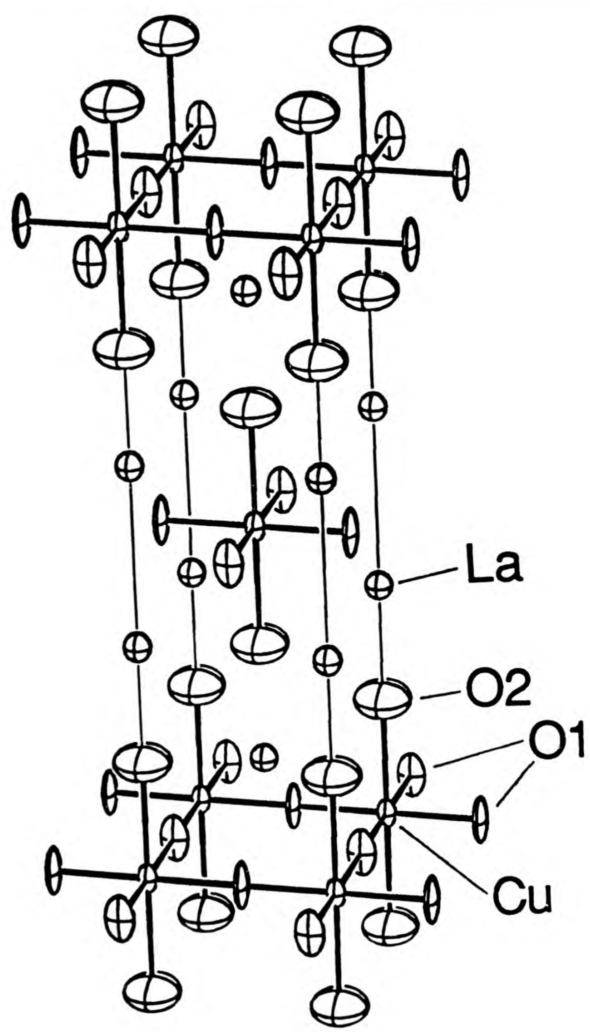

plane Cu2 atoms are 5-fold coordinated in a (very slightly distorted) square-pyramidal configuration. The oxygen designations are: O1 for in-chain, O2 and O3 for in-plane, and O4 for the oxygen above and below the chain Cu1 atom. The Cu1-O4 distance is significantly shorter (by 0.1 A) than the other CuO distances in this structure.

Local Deviations from the Average Structure

The previous section was designated "average" crystal structure because the Reitveld refinements of elastic neutron diffraction data indicate substantial local deviations from the average structure. These deviations lead to diffuse scattering which are represented as large and anisotropic "thermal ellipsoids." In well-ordered harmonic materials these ellipsoids reflect the dynamic excursions of the atoms and are strongly temperature dependent. For several of the atoms in the cuprates under consideration here, however, these thermal ellipsoids are unusually large, extremely anisotropic and nearly independent of temperature. The latter fact indicates that the displacements of the atoms from their ideal positions are static or quasi-static. As a result there is large local disorder, and it is even possible that particular atoms spend negligible time on the ideal lattice position due to a minimum in the potential somewhat off the "lattice site."

In La_2CuO_4 in the tetragonal (high T) phase, the thermal ellipsoids are pancake shaped for the La and both type of oxygens[11] as shown in Figure 3. The La ellipsoid has not been shown in this figure. For the La and O_z atoms the pancake is parallel to the layers; these atoms display large "excursions" from the ideal sites parallel to the planes which appear to be

Figure 4

Total and local densities of states of pure La_2CuO_4 (left) and of the 50% ordered Ba substitution $LaBaCuO_4$ (right). Note the marked shift in weight toward E_F (taken as zero) for the oxygen atoms near Ba ($O_{x,y}$, O_{Ba}).

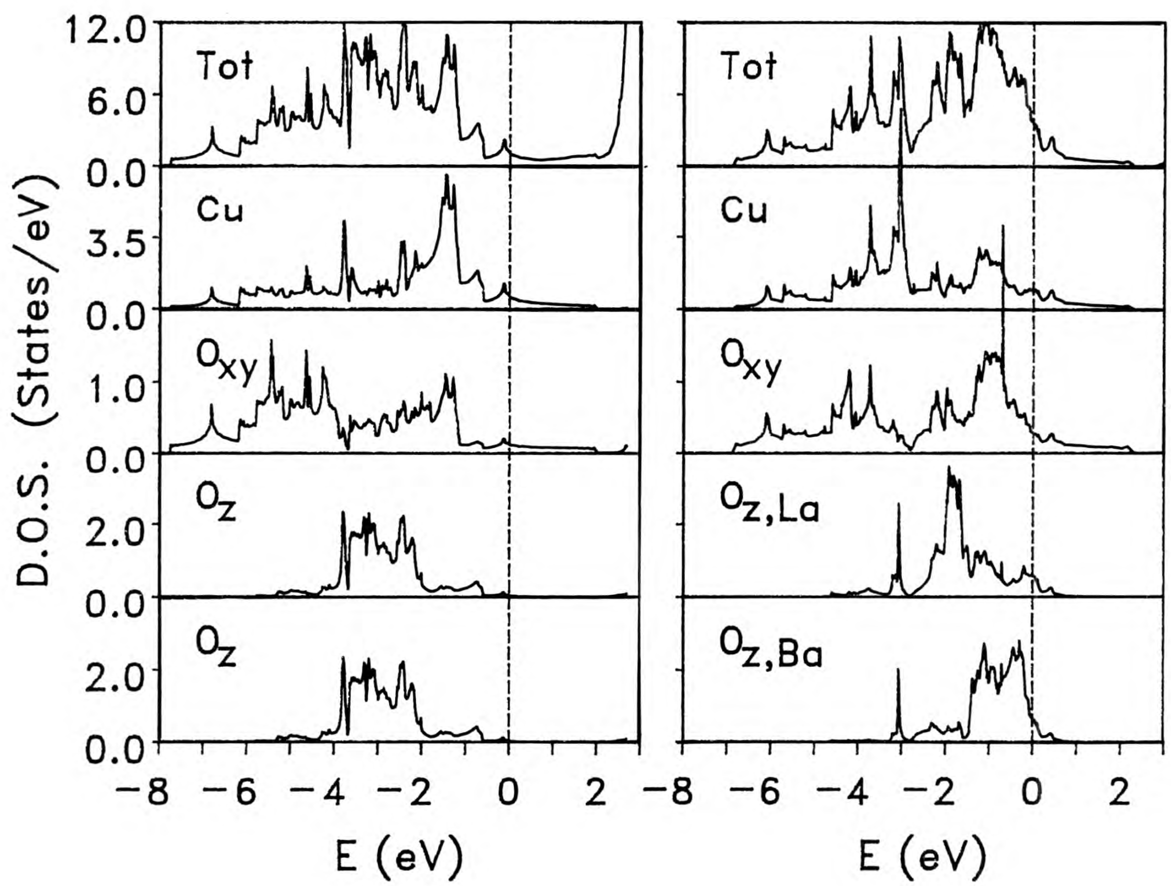

Figure 5

Bands near the Fermi level in $YBa_2Cu_3O_7$. Chain states and layer states are emphasized in the separate frames. Note that most of the states at and just below E_F are associated with the Cu-O chains.

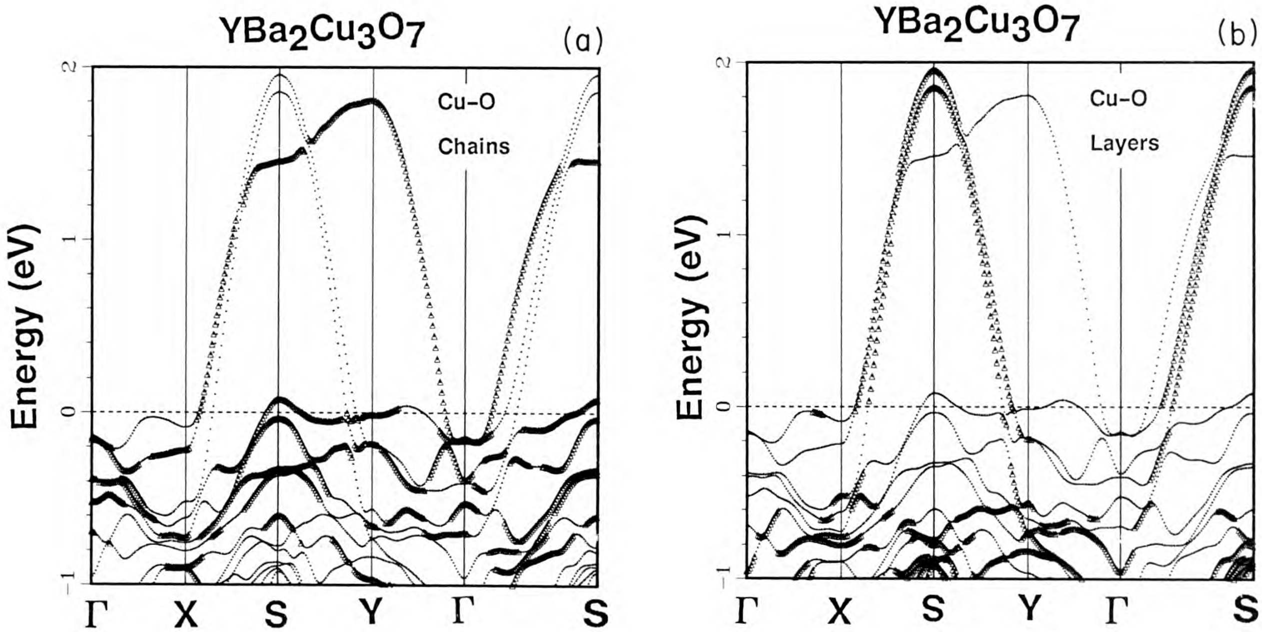

(quasi)static. The $O_{x,y}$ pancakes are oriented perpendicular to the two nearest neighbor Cu atoms; this indicates that in-plane oxygen vibrations (such as the breathing mode) are low amplitude and therefore high frequency.

Since it is not central to the discussion which follows, I will not digress into the character of the thermal ellipsoids. It is worth noting that in both materials an increase in oxygen vacancies shows up clearly in the diffuse scattering, reflecting atomic displacements ("relaxations") around the oxygen vacancies.

Bonding, Banding and Alloying

The maximum T_c is not reached in the 2-1-4 system until La is alloyed with about 7.5% Ba or Sr (x=0.15). In an effort to understand this fact, we carried out self-consistent Linearized Augmented Plane Wave studies of $LaBaCuO_4$ as well as La_2CuO_4 [NRL1]. A comparison of the density of states function of both materials in the region of Fermi energies corresponding to x=0.0 to x=0.2 indicated that *in this region alone* a rigid band model of the band structure and density of states is a reasonable first approximation. Although this assumption has been made by other band structure practitioners[12,13], none had bothered to try to verify it. Our verification is very important since, as several others have noted, applying the rigid band model indicates that the Fermi level density of states $N(E_F)$ peaks strongly at x=0.15 (it is however still quite small compared to previous "high T_c" materials). Thus the band picture predicts that T_c should be maximum at x=0.15, in beautiful agreement with experimental data. This observation, which provides strong evidence of the validity of band theory, holds almost independently of the pairing mechanism, since a larger $N(E_F)$ leads to a larger number of electrons to form Cooper pairs.

Another effect of alloying with Ba (or equivalently, Sr) could be seen in the local DOS shown in Figure 4 for both undoped and doped materials. For O ions near the Ba impurity, the local DOS was shifted strongly to smaller binding energy. This result, which is primarily an electrostatic effect resulting from the replacement of the La^{3+} with the Ba^{2+} ion, indicates that the oxygens near the Ba will be much more polarizable, their force constants will be altered, and local distortions will therefore occur around the impurity Ba ions. Evidence of such distortions has been seen in comparison of neutron diffraction data between pristine and doped samples[14].

The "doping" of cuprates by varying the concentration of O vacancies, which is easy to accomplish experimentally often over extended composition ranges, can be considered as the alloying of oxygen with oxygen vacancies. Although a rigid band model has been suggested for this situation[15], it is almost certain not to accurate, even qualitatively. Firstly, the oxygen ion presents an extremely strong electronic potential, since it manages to bind an excess of roughly two electrons in the crystal. The replacement of this strong potential by a very weak potential corresponding to a vacancy will produce strong local changes in the electronic charge and in the bonding, rather than simply contribute a small overall change to the average band potential. The rigid band picture is useful only when the replacement is isoelectronic or nearly so (e. g. Ba^{2+} for La^{3+}). Secondly, a vacancy amounts to the replacement of a 2- ion with a neutral site (unless charge is trapped at the vacant site as at F centers in ionic crystals). It was noted above that replacing the La^{3+} ion with the very similar in size Ba^{2+} ion already creates local distortions. The introduction of an O vacancy not only changes the local charge by 2 electrons but also completely eliminates the strong Cu-O short-range interactions which are crucial in determining interatomic distances. Thus very strong local distortions can be expected in the neighborhood of O vacancies, a second effect which will tend to invalidate the rigid band picture. We are currently investigating the effect of O vacancies within both self-consistent local density and parameterized tight-binding approaches.

The salient features of the band structure of the 2-1-4 system are these. The Cu-O interactions give rise to a complex of Cu(d) -O(p) bands 10 eV wide. In distinction to most transition metal oxide compounds where the O(p) bands lie well below the d bands of the metal, in this system the centers of the Cu(d) and O(p) bands exactly coincide [12]. Due to this feature and to the small Cu-O distance of 1.9 A, the hybridization is large, hence the large bandwidth. The Fermi level crosses a single band, with antibonding pd character, and leads to a Fermi surface which can be characterized roughly as a square cylinder with rounded edges. This conduction band

Figure 6

Plot of the logarithm of the valence density of La_2CuO_4 in the (100) and (110) planes. The density is very low around the La ions and between neighboring out-of-plane oxygen ions.

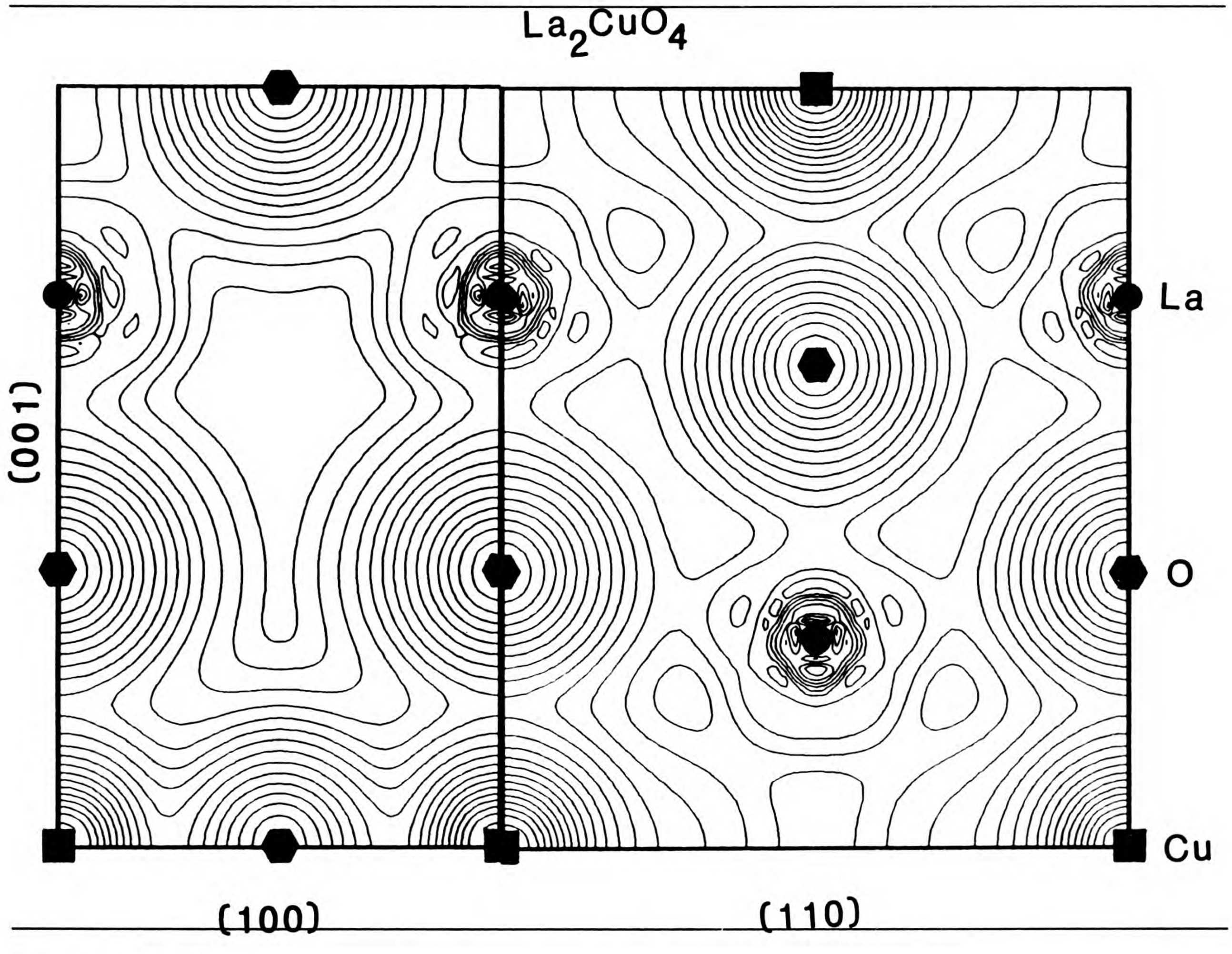

Figure 7

Plot of the valence density of $YBa_2Cu_3O_7$ in three high symmetry planes, the last of which contains the Cu-O chains. Note that the density is extremely low away from the Cu-O networks.

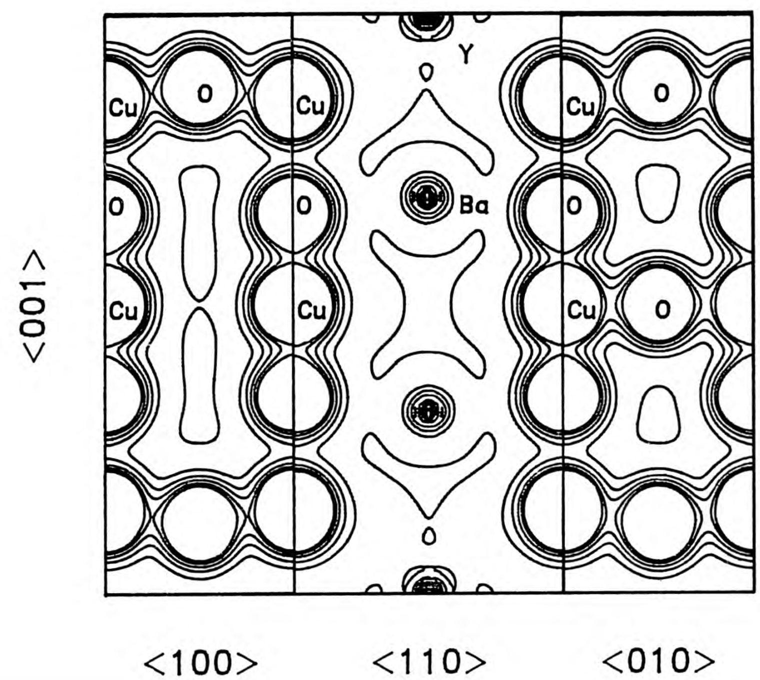

is half-filled which, due to the complexity of bands just below E_F, is most easily seen by noting that it is in fact *exactly half-unfilled.* This Fermi surface leads to strong nesting of wavevector Q at the zone boundary along the <110> directions, a point we return to later.

The alloying of La with Ba or Sr now can be seen to have yet another important influence on the properties of this system. Using the rigid band picture, alloying will lead to a lowering of the Fermi energy with respect to the pristine compound. A result of this is to reduce the Fermi surface nesting, and thereby to decrease the tendency toward a (110) lattice instability. This effect has been verified experimentally. Although the orthorhombic distortion remains in the high T_c x=0.15 alloy (earlier reports had indicated a tetragonal structure), its magnitude is decreased by an order of magnitude over that of the x=0.0 compound.

Whereas the band structure of the 2-1-4 materials has a single, roughly half-filled band crossing the Fermi level, the band structure of the 1-2-3-O_7 material is more complicated near E_F. This region of the band structure is shown in Figure 5. In addition to two Cu2-O2-O3 plane-related bands which are similar to the antibonding pd band in the 2-1-4 system, there are two Cu1-O1-O4 chain-derived bands which cross E_F. One is a broad antibonding pd band which has dispersion only along the chain direction, while the other is a pd band with rather little dispersion in any direction. An important difference between the two materials is that the bands crossing E_F in the 1-2-3 system are *not close to being half-filled.* The Fermi surfaces, which can be characterized as approximately one-dimensional (for the chain bands) or two-dimensional (for the plane bands) do however present significant nesting features, but they correspond to several distinct incommensurate Q vectors. This fact may account for the apparent lack of strong antiferromagnetic tendencies of structural instabilities in the 1-2-3 system such as are seen in the 2-1-4 material (discussed below). The total Cu-O band complex is nearly as wide as in the 2-1-4 system.

An unusual feature of the electronic structure of these cuprates is evident from the calculated charge density, shown in Figures 6 and 7 for the 2-1-4 and 1-2-3 systems, respectively. While the Cu-O networks have strong wavefunction overlap leading to metallic-like density within the networks, the regions around the La, Ba and Y ions and in the interstices are almost devoid of valence density. The resulting combination of ionic and metallic characters will lead to novel electronic and lattice behavior which we have only begun to unravel.

Transport Properties - Hall Coefficient and Thermopower

We have calculated several quantities related to the d.c. transport properties of both cuprate systems. These properties, such as the conductivity, thermopower S and the Hall coefficient R, depend on the value of $N(E_F)$ as well as averages over the Fermi surface of expressions involving band velocities (first derivative of E_k) as well as the inverse band mass tensor (second derivative of E_k). Also some assumption must be made about the scattering processes, and different models for the relaxation time have been tested. The details are not relevant here, except to note that it has been necessary to develop a more precise Fourier series representation of the bands [NRL10] to allow an accurate evaluation of the inverse band mass tensor.

In the 2-1-4 alloy system, experiments on polycrystalline samples usually find the Hall coefficient to be hole-like, although considerable differences in magnitude (and occasionally in sign) have been reported. The band picture predicts strong anisotropy, which makes data on single crystals almost indispensible for meaningful comparison. The band predictions are as follows. As for the Hall coefficient [NRL2], it is found to be hole-like for magnetic field H perpendicular to the planes, in which case the carriers move in the layers. This behavior is illustrated in Figure 8. For field directions in the plane, however, R is found to be *electron-like*. A single crystal measurement (for x=0.06) by Suzuki and Murakami[16] for the perpendicular field direction gave a hole-like result, consistent with our calculations, and a value at 300 K (where the calculated value is most appropriate) a factor of 2.6 larger than theory. Since similar discrepancies have been seen in Pd and can be ascribed to approximations made in the calculational theory, this level of agreement can be considered very encouraging. Another unusual prediction of the calculations is that the sign of R for perpendicular field should change sign around the alloy concentration of x=0.24.

We have also calculated [NRL5] the thermopower S (Seebeck coefficient), which has independent components within and perpendicular to the basal plane. S depends on the energy dependence of the conductivity near the Fermi level, and like R should provide a clear test of the band picture when compared to single crystal data. Regardless of the assumptions we make about the scattering mechanism (three models were tested), moderately large positive "hole-like" behavior is obtained for conduction perpendicular to the layers while smaller negative "electron-like" behavior results for conduction in the planes. It is notable that the "sign of the carriers" not only changes sign for the different orientations, as was found for R, but the sense is opposite to that of R: for carrier motion in the plane R is "hole-like" while S is "electron-like", and vice-versa for motion perpendicular to the plane. These predictions are in *drastic qualitative distinction* to a picture of a small concentration of holes with an ellipsoidal Fermi surface, which would show only hole-like behavior for any orientation and for both R and S. A "two band model" could perhaps be constructed which would emulate the qualitative predictions of our detailed band model, however.

We have also calculated the corresponding transport properties of the 1-2-3 material [NRL11], and there is already one experimental result which strongly supports our calculations and therefore the band picture. We find that the Hall coefficient should be hole-like for field perpendicular to the planes, and that it should be electron-like with two different values for the two independent field directions in the plane. Tozer et al.[17] have measured R on a highly twinned "single crystal." For the field perpendicular to the layers they found a hole-like sign, as expected from ceramic data obtained previously by many groups. For the field oriented parallel to the layers, they obtaining an electron-like sign with value midway between the two in-plane theoretical values, just as would be expected for a twinned crystal from our calculations.

Figure 8

Representative results versus alloy concentration x for transport-related quantities in $La_{2-x}M_xCuO_4$ materials. R_{ijk} denotes the Hall tensor with the magnetic field in the k-direction. The density of states and the two distinct components of the Drude plasma energy are shown below.

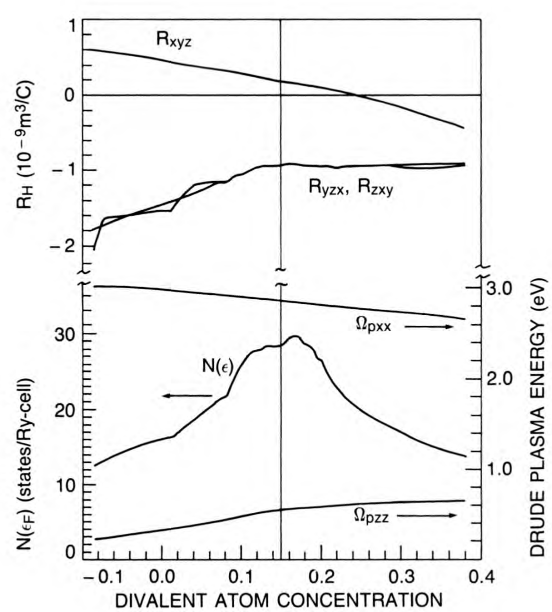

Figure 9

Shift in the valence charge density (above) and the one-electron potential (below) in La_2CuO_4 due to a displacement of O_z atoms in the axial breathing mode.

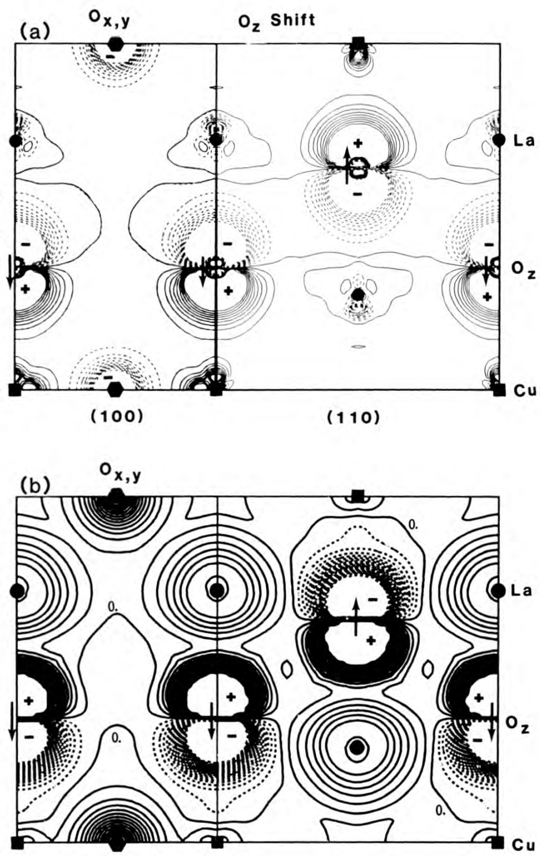

Anisotropy of the Band Velocities and Resistivity

The most fundamental characteristic in understanding the transport properties of a system, other than the scattering properties, is the quasiparticle velocity $v_k = dE_k/dk$. In a vast majority of metals the local density bands provide excellent bands and velocities, although in principle a complicated self-energy correction is involved. In the Hall coefficient and thermopower discussed above, the velocity plays a central role, as it also does in the d.c. and a.c. conductivity. Both the d.c. and the low frequency a.c. conductivity depend on the "Drude plasma energy", which is proportional to the Fermi velocity times the square root of $N(E_F)$.

The large anisotropy evident in the crystal structure and the band structure is reflected in the Fermi velocity, which is different in the plane and perpendicular to it due to the low symmetry. For x=0.15 in the 2-1-4 system, the Fermi velocities [NRL2] differ by a factor of 5, being 2.2 in-plane and 0.41 perpendicular, in 107 cm/sec. The corresponding values of the plasma energy tensor are 2.9 eV in-plane and 0.55 eV perpendicular. These results immediately suggest that the resistivity will be a factor of $5^2=25$ lower perpendicular to the layers than in-plane, unless the scattering processes are much different in the two directions.

Electron-Phonon Coupling and T_c

There has been much speculation about the role, or lack thereof, of the electron-phonon interaction (EPI) in pairing electrons in these novel high T_c materials. Experimentally, the isotope effect is the main indicator of the involvement of phonons in pairing, and the results are now in:[18] within rather small limits there is zero isotope effect in the 1-2-3 system, while there is a rather substantial oxygen isotope effect in the 2-1-4 system. Thus the EPI is definitely involved in pairing in the 2-1-4 system, while in the 1-2-3 compounds the phonons are "invisible." This latter effect can be accounted for by an electronic mechanism which is separate of the phonons, or by an unusual EPI which results in drastically reduced or zero isotope shift of T_c.

Using an approach which has proven very successful for transition metal elements and carbonitrides and for the A15 compounds, we have evaluated the strength of the EPI in both cuprate systems. This approach is a rigid-atom-type method called the rigid muffin-tin approximation. It is most appropriate in compounds where the atoms scatter electrons strongly at the Fermi level, which is certainly the case for the Cu and O atoms in these cuprates. It also assumes that the change of potential due to the motion of an ion is small except near that ion, i. e., that the screening length is small. This assumption is suspect in these mixed ionic-metallic systems, a point which I will return to below.

In both systems the calculated EPI strength λ is dominated by the contributions from the oxygen ions. In the 2-1-4 system with x=0.15 (where T_c is maximum) the calculated strength is between 2 and 4, depending rather strongly on what the mean phonon frequency which enters in Eliashberg theory is assumed to be. The calculated T_c is much less sensitive to the assumptions about the frequency spectrum, however, and for perhaps optimistic but reasonable frequencies the calculated T_c lies in the 30-40 K range. This is certainly encouraging, and led us to predict [NRL1] that the EPI interaction is central to superconductivity in the 2-1-4 system, before the isotope effect results were reported and confirmed the predictions.

In the 1-2-3 system the calculated strength [NRL11,NRL12] of the EPI was found to be *25% less* than in the 2-1-4 system, as long as the phonon spectrum is similar. Although this coupling is still "strong" in the pre-1987 sense, it cannot come anywhere close to accounting for T_c in the 90 K range. Again, our calculations are consistent with the isotope effect measurements, and appears to indicate a non-phonon pairing mechanism of this system.

There are, however, strong indications that this is not the full story concerning the EPI. First, we have learned from our local density LAPW calculations that there is an unusual type of EP coupling in the 2-1-4 system that arises from the mixed ionic-metallic character. The change in charge density due to the axial breathing mode, in which the two out-of-plane oxygens move along the c-axis, is shown in Figure 9. Other than the rigid-ion-like shift of the oxygen itself, this mode results in a movement of charge between the Cu and in-plane oxygen. In other words, the movement of one atom results in charge movement from a second atom to a third. This effect is negligible in "ordinary" superconductors, and is ignored both in the calculations of Weber[19] and in our rigid muffin-tin calculations discussed above. It is the result of a shift of the Madelung potential due to the displacements involved in the axial mode: the electron potential on both the in-plane oxygen and on the La is strongly affected. Since there is little valence charge on the La, its participation appears to be slight, but a large movement of charge on and off the $O_{x,y}$ may alter the character of the EPI considerably.

A second point is that in all calculations carried out so far, it has been assumed that the equilibrium position of the atoms is the ideal lattice site, whereas the "thermal ellipsoids" from the neutron scattering experiments, discussed in Sec. III, indicate that the atoms, except for the Cu, deviate strongly from the ideal sites. Unless there is extremely large anharmonicity, which does not seem likely due to the near T-independence of the phonon density of states, it is likely that the equilibrium positions of the atoms lie well off the ideal lattice sites, and there is considerable short-range disorder. In such a case a proper description of the lattice dynamics and EPI is not only greatly complicated but could be altered qualitatively.

Lattice Statics/Dynamics: An Ionic Description

The mixed ionic-metallic character of these copper oxides poses a new challenge to understand not only the electronic excitations but also the structural instabilities and lattice dynamics. We have found that the ionic character leads to qualitatively different static response to ionic displacements than is normal in the previously studied "high temperature" superconductors, such as the transition metal carbonitrides and A15 compounds.

The "standard" metallic description of lattice dynamics has been applied to La_2CuO_4 in considerable detail by Weber[19]. His method consists of fitting a parametrized tight-binding Hamiltonian to the *ab initio* band structure of Mattheiss[12]. The band structure energy (the eigenvalue sum) is used to determine the many-atom forces which can be long-range in nature because of Fermi surface effects, while short-range repulsive force constants are obtained in a less rigorous fashion. The band structure energy contains contributions from three-center terms and two-center terms of an ionic nature which are neglected because they are unimportant in high density metals where the screening length is short. Furthermore, the residual forces may have considerable ionic character and may not simply be short-range, as he has assumed. Weber's primary conclusion was the prediction of a soft oxygen Q=(110) breathing mode for x decreasing from 0.2, becoming unstable in the pristine compound. Unfortunately for this approach, the symmetry of the instability is different than what is observed, and the soft breathing mode is not observed[7].

We have tested an ionic description of structural and dynamical properties of La_2CuO_4 by applying the Potential Induced Breathing (PIB) model of Boyer and collaborators[20]. In this approach the density of the solid is approximated by overlapping spherical ionic densities, each calculated within the local Madelung potential of the crystal. This latter feature is crucial for the O^{2-} ion which is only stable within an ionic solid. The energy of the system is obtained from local density expressions for the kinetic energy as well as for the exchange-correlation energy. The PIB approach has given surprisingly accurate results for several classes of ionic crystals for the

Figure 10

Difference between the crystalline LAPW charge density and the PIB ionic model density, showing the charge rearrangement in the Cu-O plane. The solid contours around the La and O_z atoms denote zero difference.

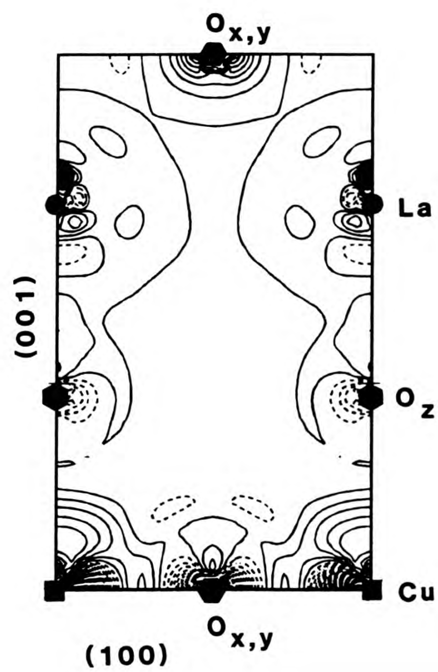

Figure 11

Calculated phonon spectrum of La_2CuO_4 in the tetragonal (a) and orthorhombic (b) structures. Negative frequencies denote harmonically unstable modes. In (a) the most unstable mode at X is the rotational mode (about the c-axis) of the CuO_6 octahedron, while the second most unstable is the octahedral tilt mode which freezes into the lattice at the structural transformation. The dispersionless unstable mode in both structures involves sliding motions of the O_z and La atoms parallel to the planes.

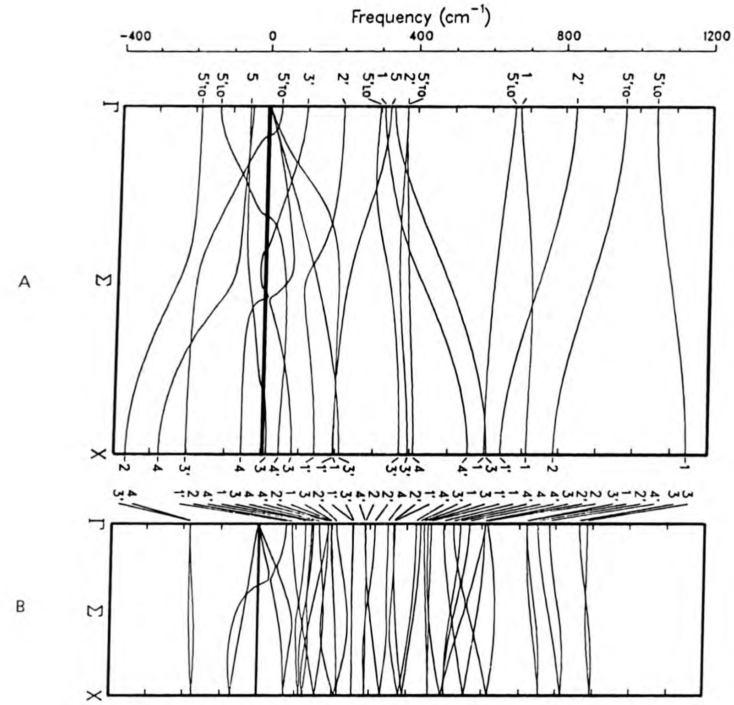

equation of state, structural energy differences, lattice dynamics and the like, but has not previously been applied to a material as polarizable as this 2-1-4 compound.

This ionic model has been applied for two situations, restricting the space group to be tetragonal I4/mmm in the first case, and to orthorhombic Abma with two formula units in the second case. The choice of ionic configurations was La^{3+}, O^{2-} and (sphericalized) Cu^{2+}. The predicted static tetragonal structure differs from the experimental one by having a cell volume 5% too large and a c/a ratio 15% too large, but the internal structural parameters are predicted well. The primary difficulty with the ionic picture is that it is energetically unfavorable for spherical O and Cu ions to lie as close together in-plane as occurs in the 2-1-4 system. In the crystal considerable distortion of the oxygen ion and especially the Cu ion occurs, as can be seen from Figure 10 which shows the difference between the crystalline LAPW density and the PIB density [NRL3]. The La and O_z ions are described very well as fully ionic, however. It is worthy of note that the distortion of the CuO6 octahedron, which is usually described in terms of a Jahn-Teller instability of the unfilled Cu d shell, is obtained within a purely ionic picture, although the magnitude of the distortion is underestimated by about a factor of two.

The calculated phonon spectrum is displayed in Figure 11a, where negative frequencies denote harmonically unstable frequencies. The O breathing mode, which lies at the (110) zone boundary, is the *hardest mode* here, rather than being the softest as in Weber's calculation. The most unstable mode is the rotation of the octahedra around the c-axis (a mode which is often soft in perovskite-like structures), while the second most unstable mode is the tilt mode which inelastic neutron scattering measurements have verified is the one frozen into the lattice at the structural transition. The other strongly unstable mode is the nearly Q-independent sliding mode involving O_z and La atoms moving parallel to the planes. The flatness of this mode reflects a completely uncorrelated motion in the x-y plane of these atoms, which accounts for the thermal ellipsoid "pancakes" seen in the structural refinements.

When the space group is relaxed to Abma, the rotation of the CuO_6 octahedrons (shown in Figure 12) that is seen experimentally results, although the angle obtained is considerable larger than the experimental value of 5 degrees. This overestimate again reflects the strong short-range repulsion between spherical ions, which is no doubt decreased by non-spherical distortions. The "negative distortion"[14] a>b is also obtained; rigid Cu-O bond lengths would result in a<b. The phonon spectrum is shown in Figure 11b. The tetrahedrally-unstable rotational and tilt modes are folded back to the zone center and become stable, and the maximum frequency decreases strongly, to within 10% of the experimental value. The primary remaining instabilities are an elastic instability and the sliding $La\text{-}O_{x,y}$ mode. This PIB ionic description predicts a yet lower symmetry ground state, probably of monoclinic symmetry, and there are experimental indications of such a transformation in some samples[21,22].

Band Picture vs. Highly Correlated Picture

Except for the lattice statics/dynamics covered in the previous section, our studies have been aimed at providing detailed numerical tests of the band picture in comparison with direct experimental data. Although there are many encouraging points of agreement which indicate the band picture is realistic, there are several items which raise clear questions. An alternative to the local density band picture has been proposed by a number of workers, to wit: the new cuprates are Mott insulators which are doped with carriers either by alloying on the cation site, or by the introduction of oxygen vacancies, or both. Usually the Mott instability is attributed to a strong on-site Coulomb repulsion involving the Cu d states. Here I will mention and discuss briefly a few possible problems with the band picture.

The most obvious discrepancy between the band structure and experimental data is for pristine La_2CuO_4. The band structure indicates it should be a good, although "low density," metal. The measured resistivity, however, is non-metallic, that

Figure 12

Pictorial representation of the tilt mode which is soft in the tetragonal phase of the 2-1-4 structure and freezes into the lattice at the orthorhombic transformation around 500 K.

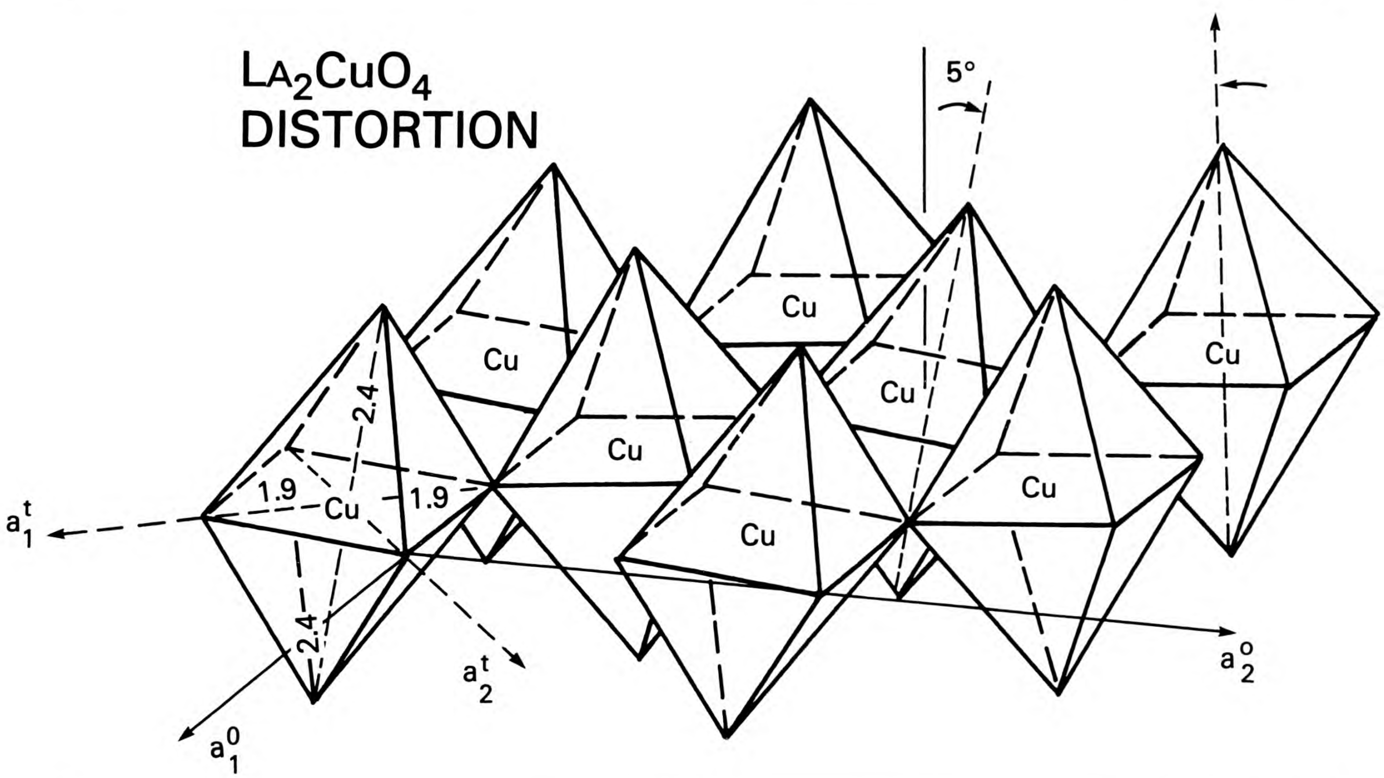

is, it increases with decreasing temperature. It is not fit well by an activated form, which makes it impossible to identify a band gap. The data are usually interpreted qualitatively in terms of a doped semiconductor, but recent measurements on single crystals of undoped 2-1-4 and an x=0.04 (Sr doped) sample have provided new evidence. Birgeneau et al.[9] found that the log of the resistivity followed a $(T_o/T)^{1/4}$ form from above 400 K down to 10 K. This form is of the "variable range hopping" type suggested theoretically for highly disordered (Anderson localized) systems. Although a doped semiconductor conceivably could give rise to such behavior, another possibly can be considered. The system could have no true gap to single-particle excitations, but due to either strong (one-electron) disorder or to strong (many-body) interactions (or both), the states at the Fermi level become localized. The "thermal ellipsoids" seem to indicate strong disorder which could tend to push the Fermi level states toward localization, especially if the states are heavily oxygen-related.

It may be noticed that I have not compared the band density of states with the numerous photoemission experiments which have been carried out. Although the detailed interpretations differ considerably from group to group, a widespread conclusion is that "band theory puts the Cu d states too close to the Fermi energy," by 1 eV or so. There are two strong reasons to be wary of this comparison as a strong argument against the band picture. The first relates to the extreme surface sensitivity of the photoemission experiment, which samples states which are typically 20 to no more than 40 A below the surface. Gray[23] has noted that researchers carrying out point-contact tunneling must push the sharp "contact" several hundred Angstroms into the crystallite to find metallic material; the crystallites are surrounded by a shell of insulating material. Thus it is very likely that the photoemission spectra is not representative of the bulk superconducting material. The second point is that, even if the band picture underestimates the binding energy of the more-or-less non-bonding Cu d states which contribute to the large density of states peaks somewhat below E_F, the wide-band Cu-O states which cross E_F will be more band-like and therefore less affected by correlations which increase the binding energy over the band value. Thus an error in the binding energy of a density of states peak *below* E_F does not necessarily invalidate the band picture of the states *crossing* E_F.

Another apparent difficulty with the conventional band picture is the occurrence of antiferromagnetism in La_2CuO_4. Several practitioners[24] have found that local spin density theory, which has been highly successful in describing band magnetism in a variety of systems, not only does not predict an AFM state, but also does not indicate any strong tendency toward magnetism. Although this must remain a concern, the implications of these null results remain uncertain. First, as pointed out above, there is considerable local disorder in the 2-1-4 system, and this has not been accounted for in the calculations. Second, the occurrence of the AFM state is strongly dependent on the O vacancy concentration.

Gurvitch and Fiory[25] have pointed out a difficulty with the explanation of the linear resistivity as due to the EPI. Using the band prediction for the band velocity and density of states, the EPI strength necessary to account for the temperature dependence of the resistivity leads to a violation of the Ioffe-Regel criterion, that is, the mean free path is less than an interatomic spacing. In this regime standard transport theory is no longer valid, and in nearly all metals where the Ioffe-Regel limit is approached the resistivity is seen to saturate. No saturation occurs in either the 2-1-4 or 1-2-3 systems. This criticism is less one of the implied EPI strength than of the band structure itself; if the Drude plasma energy from band theory were a factor of 3 to 5 smaller, the implied mean free path would no longer violate the Ioffe-Regel criterion, and saturation would not be expected. A strongly wavevector-dependent self-energy could act to lower the velocity and therefore the Drude plasma energy of the quasiparticles (which than would differ from the band description) but, since the plasma energy is much less sensitive than either the DOS or the Fermi velocity, a very large self-energy correction would be required.

Summary

The work described here represents only the initial phase of a theoretical program to describe the normal state properties, and later the superconducting properties, of the remarkable new high T_c copper oxides. Only the results necessary to give a general viewpoint have been presented and discussed; the original papers should be consulted for more details.

In this brief review I have not tried to address in any detail the complex role of many-body effects, i. e., beyond the local density approximation, which already have been the subject of a large number of papers concerning these cuprates and their superconductivity. A few of the (apparent) shortcomings of the band picture have been discussed, and these suggest the possible importance of correlation effects. On-site Coulomb correlation integrals (Hubbard U's) for both Cu and O can be calculated within LDA, and there now exist several model forms of single-particle self-energy functions which can be applied to investigate dynamic correlation effects. Unlike the heavy fermion and mixed valent systems, however, it is unlikely in these cuprates with their strong hybridization that the intra-site Coulomb interaction will completely dominate the inter-site Coulomb interaction. If this indeed is the case, the simple (i.e. without extended Coulomb interaction) Hubbard model treatments will be too simple to model their properties.

Epilogue

It should be kept in mind that this report of the first year's theoretical work at NRL was written at the end of 1987. Although it has been checked for accuracy of experimental facts as of January 1989 (necessitating a few changes) no attempt has been made here to bring this discussion up to date. A fairly comprehensive review of the understanding of the electronic structure of copper oxide superconductors through 1988 will appear in the April 1989 issue of Reviews of Modern Physics [NRL14]. This review contains over 350 references to the literature of the electronic structure of cuprate superconductors, including the more recent work of our NRL group.

Biography

Dr. Pickett is a research physicist in the Complex Systems Theory Branch at the Naval Research Laboratory. His research and publications are mainly in the fields of electronic structure of solids and electron phonon interactions in metals. Dr. Pickett published recently in *Reviews of Modern Physics*, Vol. 61, page 433, 1989, "Electronic Structure of the High Temperature Oxide Superconductors," which is an expanded version of the article that appears here.

References: NRL Theory papers

[NRL1] W. E. Pickett, H. Krakauer, D. A. Papaconstantopoulos and L. L. Boyer, Phys. Rev. B*35*, 7252 (1987). "Evidence of Conventional Superconductivity in La-Ba-Cu-O Compounds."

[NRL2] P. B. Allen, W. E. Pickett and H. Krakauer, Phys. Rev. B*36*, 3926 (1987). "Band Theory Analysis of Anisotropic Transport in La_2CuO_4-based Superconductors."

[NRL3] W. E. Pickett, H. Krakauer, D. A. Papaconstantopoulos, L. L. Boyer and R. E. Cohen, in *High Temperature Superconductors*, edited by D. U. Gubser and M. Schlüter (Mat. Res. Soc., Pittsburgh, 1987), 31. "Electronic Structure, Bonding and Electron-Phonon Interaction in La-Ba-Cu-O Superconductors."

[NRL4] H. Krakauer and W. E. Pickett, in *Novel Superconductivity*, edited by S. U. Wolf and V. Z. Kresin (Plenum, New York, 1987), 501. "Character of States near the Fermi Level in $YBa_2Cu_3O_7$."

[NRL5] P. B. Allen, W. E. Pickett and H. Krakauer, in *Novel Superconductivity*, edited by S. U. Wolf and V. Z. Kresin (Plenum, New York, 1987), 489. "Prediction of Anisotropic Thermopower in $La_{2-x}M_xCuO_4$."

[NRL6] D. A. Papaconstantopoulos and L. L. Boyer, in Novel Superconductivity, edited by S. U. Wolf and V. Z. Kresin (Plenum, New York, 1987), 493. "Band Structure and Electron-Phonon Interaction Calculations for Proposed High-T_c Superconducting Oxides: $MCuO_3$ (M=La, Ba, Cs, Y) in the Perovskite Structure."

[NRL7] H. Krakauer, W. E. Pickett, D. A. Papaconstantopoulos and L. L. Boyer, Jpn. J. Appl. Phys. **26**, 991 (1987). "High Temperature Superconductors: Electronic Structure Changes due to Replacement of La with Ba and Sr in the Cu-O - based Systems."

[NRL8] D. A. Papaconstantopoulos, W. E. Pickett, H. Krakauer and L. L. Boyer, Jpn. J. Appl. Phys. **26**, 1091 (1987). "Calculations of the Superconducting Properties of Cu-O Based Perovskite-like Structures."

[NRL9] R. E. Cohen, W. E. Pickett, H. Krakauer and L. L. Boyer, Physica B 150, 61 (1988). "Applications of Ionic Models to the High Temperature Superconductor La_2CuO_4."

[NRL10] W. E. Pickett, H. Krakauer, and P. B. Allen, Phys. Rev. B**38**, 2721 (1988). "Smooth Fourier Interpolation of Periodic Functions."

[NRL11] P. B. Allen, W. E. Pickett and H. Krakauer, Phys. Rev. B**37**, 7482 (1988). "Anisotropic Normal State Transport Properties Predicted and Analyzed for High-T_c Oxide Superconductors."

[NRL12] H. Krakauer, W. E. Pickett, and R. E. Cohen, J. Supercond. **1**, 111 (1988). "Analysis of Electronic Structure and Charge Density of the High Temperature Superconductor $YBa_2Cu_3O_7$."

[NRL13] R. E. Cohen, W. E. Pickett, L. L. Boyer and H. Krakauer, Phys. Rev. Lett. **60**, 817 (1988). "Ionic Contributions to Lattice Instabilities and Phonon Dispersion in La_2CuO_4."

[NRL14] W. E. Pickett, Rev. Mod. Phys. **61**, 433 (1989). "Electronic Structure of the High-Temperature Oxide Superconductors."

References: Other Papers

1. G. Bednorz and K. A. Müller, Z. Phys. B64,189 (1986).

2. C. W. Chu et al., Phys. Rev. Lett. *58*, 405 (1987).

3. J. Bardeen, L. N. Cooper and J. R. Schrieffer, Phys. Rev. *106*, 162 (1957); ibid. *108*, 1175 (1957).

4. B. N. Brandow, Adv. Phys. *26*, 651 (1977).

5. V. B. Grande, Hk. Müller-Buschbaum and M. Schweizer, Z. Anorg. Allg. Chem. *428*, 120 (1977).

6. J. D. Jorgensen et al., Phys. Rev. Lett. *58*, 1024 (1987); P. Day et al., J. Phys. C*20*, L429 (1987).

7. R. Birgeneau et al., Phys. Rev. Lett. *59*, 1329 (1987).

8. D. Vaknin et al., Phys. Rev. Lett. *58*, 2802 (1987).

9. R. Birgeneau et al., Phys. Rev. B*38*, 6614 (1988).

10. M. A. Beno et al., Appl. Phys. Lett. *51*, 57 (1987); F. Beech et al., Phys. Rev. B*35*, 8778 (1987); J. D. Jorgensen et al., Phys. Rev. B36, 5713(1987).

11. J. D. Jorgensen et al., Phys. Rev. Lett. *58*, 1024 (1987); J. D. Jorgensen, private communication.

12. L. F. Mattheiss, Phys. Rev. Lett. *58*, 1028 (1987).

13. J. Yu and A. J. Freeman, Phys. Rev. Lett. *58*, 1035 (1987).

14. J. D. Jorgensen, private communication.

15. S. Massidda et al., Phys. Lett. A*122*, 198 (1987).

16. M. Suzuki and T. Murakami, Japanese J. Appl. Phys. *26*, L524 (1987).

17. S. W. Tozer et al., Phys. Rev. Lett. *59*, 1768 (1987).

18. T. A. Faltens et al., Phys. Rev. Lett. *59*, 915 (1987); B. Battlogg et al., *ibid*. *59*, 912 (1987).

19. W. Weber, Phys. Rev. Lett. *58*, 1371 (1987).

20. L. L. Boyer et al., Phys. Rev. Lett. *54*, 1940 (1985).

21. S. C. Moss, Phys. Rev. Lett. *58*, 7195 (1987).

22. E. S. Skelton et al., Phys. Rev. B*36*, 5713 (1987).

23. K. Gray, in *Novel Mechanisms in Superconductivity*, edited by S. A. Wolf and V. Z. Kresin (Plenum, New York, 1987), in press.

24. See particularly, T. C. Leung, X. W. Wang and B. N. Harmon, Phys. Rev. B*37*, 384 (1988).

25. M. Gurvitch and A. T. Fiory, in Ref. 23.

Navy Leads In The Development Of New, Safer, Synthetic Oxygen-carrying Resuscitation Fluids

by Captain Robert E. Baier, USNR and Commander Thomas J. Contreras, MSC, USN
Office of Naval Technology

Recent events in the Persian Gulf, like the missile attack on the USS Stark, have dramatized the reality of the Navy's need for immediate response to combat casualty care under the most remote of circumstances. Alone, in the middle of a hostile ocean, each ship must be able to provide instant life-saving measures to its sailors who are wounded and in shock. This must be done, obviously, from a limited storehouse of only the most useful and universal materials, packed in minimum space and probably subject to extremes of temperature, humidity, and mechanical trauma during long difficult deployments.

What can the Navy do about its needs for blood transfusions under these circumstances? How can it assure availability of precious, oxygen-carrying fluids that are acceptable to every person aboard — regardless of blood type or possible allergies — and entirely free from toxic agents and viruses (e.g. AIDS; hepatitis)? Clearly, with its own mission readiness at stake, the U.S. Navy has had good reason to lead in the search for safe, therapeutically effective blood and blood substitutes!

Already developed and deployed, on its Hospital Ships and several of its Casualty Receiving and Treatment ships (CRTs), are Frozen Blood Bank Systems. The U.S. Navy has obtained Food Drug Administration (FDA) authorization for the freezing, 10-year storage (in the frozen state), washing (to remove the cryoprotective agent), and three day post-wash storage of red blood cells. This technology, developed at the Naval Blood Research Laboratory, Boston University School of Medicine, Boston, Massachusetts, has become the backbone of the Department of Defense Military Blood Program Office. The Frozen Blood Bank Systems will afford the Navy, and other armed forces, the capability to preposition large quantities of O+ and O- type red blood cells, overcoming some of the logistical problems associated with fresh-stored blood. Since medical readiness limitations still remain with frozen blood technology, the Navy continues its search for the definitive solution — "artificial blood". It has succeeded admirably with one exciting approach now being produced with commercial partners — synthetic red blood cells.

Advancing the concept announced by T.S. Chang in 1957 and later by Djordjevich and Miller in 1980, i.e., the creation of a "synthetic" red blood cell, the Navy's own "corporate research laboratory," the U.S. Naval Research Laboratory, has been granted a patent for the production of a synthetic red blood cell. The Navy's patent for a method allowing "Scaled-up Production of Liposome Encapsulated Hemoglobin", developed by Drs. Martha C. Farmer, Richard L. Beissinger and Bruce P. Gaber, describes a novel blood substitute that is postulated to be transfused to human patients without concern for the recipients' blood types. The promising new material results from many years of dedicated research sponsored initially by the Office of Naval Research (ONR) and currently by the Office of Naval Technology (ONT).

Significant progress has been made in the development of large-scale production procedures and methods for longterm stabilization of the new "artificial blood." The actual product is called "Liposome Encapsulated Hemoglobin" or "LEH," which is basically a preparation of the oxygen-carrying hemoglobin of real blood cells encased in much smaller fatty-like "baggies." These "baggies" or liposomes are, in fact, tiny hollow bodies ("somes") composed of simple fatty ("lipo") materials like lecithin, cholesterol, and vitamin E. There is a great deal of important research currently in progress on the use of such liposomes for carrying a variety of anti-cancer drugs to specific targets in the human body. Although successful at these small volumes, the successful use of liposome encapsulated material in the large quantities required for therapeutic effective transfusions has not yet been demonstrated.

LEH is made from hemoglobin solutions isolated from otherwise outdated whole blood. These solutions are mixed with dry batches of the selected fatty materials (usually those known to be present in natural cell membranes, like that of the red blood cell itself) and extruded at high pressure through narrow channels of a "microfluidizer." The resulting liposomes resemble red blood cells without the blood group antigens, theoretically rendering them universally acceptable for transfusions. The Navy's research has shown these LEH preparations to meet the physical and chemical criteria for an artificial oxygen transport system. Indeed, tests in small animals have been very successful, with the preparations sustaining life functions for more than a day when more than half of the animal's normal red blood cells are replaced by the LEH infusions.

What is now needed is large-scale testing of the safety and therapeutic effectiveness of these materials, produced in sterile pilot-plant equipment rather than in the experimental research laboratory. Since the U.S. Navy recognizes the urgent need existing in all military medicine for an oxygen-carrying blood substitute useful for resuscitation of battle casualties, and particularly for materials that can be stowed in a minimum of space on board ships for long periods of time, it has now further set aside funds for the preclinical evaluation/demonstration of the synthetic red cell. In the modern world, where seriousness of purpose is often spelled "money", it is serious, indeed, that the continuing Navy effort is budgeted at more than $4,000,000 between now and Fiscal Year 1992. The demonstration project will commit the resources of the Director of Naval Medicine/Surgeon General of the Navy to carry the successes of the technology base (Office of Naval Research and Office of Naval Technology) program to practical commercial levels. The specific achievement forecasted is the production of synthetic red blood cells (LEH) composed of natural lipids, blood hemoglobin, and natural stabilizers that are small enough (circa 0.2 micron) to pass into and through the smallest constricted capillaries and perform the same physiological functions as natural red cells (8 micron in diameter). These functions include having the same or superior oxygen exchange properties as red cells, with circulating half-lifes of 1-3 days, and having the same flow properties as red blood cells.

Some aspects of the production process have already been transferred to industry, where advanced liposome technology has previously been implemented in clean-room conditions (for prevention of the incorporation of pyrogens – fever producing substances) that meet all requirements of the Food and Drug Administration. Due to the shortage of human blood, a pyrogen/virus-free commercial source of large volumes of blood is essential for the success of this production process. The bioengineering of synthetic hemoglobin with excellent scale-up potential and simplified purification is imperative. Such a source has recently been identified. The introduction of this recombinant human hemoglobin biotechnology will afford the development of a undeniably synthetic red blood cell.

Researchers at the Naval Research Laboratory, Drs. Alan S. Rudolph and Frances S. Ligler, are committed to providing continuing quality control of the LEH product and addressing the issue of the long-term stability of this blood substitute. Lyophilization (freeze-drying) of LEH into a dry powder affords the greatest promise of long-term storage at any temperature.

One of the major remaining issues is to identify the proper procedures and places to ascertain the safety or "biocompatibility" of the final Synthetic Red Blood Cell product in healthy and injured individuals. To further enhance the biocompatibility and life span of LEH in humans, the Office of Naval Research has inaugurated a supporting program to modify the surface of the LEH. The surface of a normal red cell is composed of sugars that signal the reticuloendothelial system (RES) (areas within the body that are responsible for the removal of foreign material) that the cells are young and healthy. By the addition of sugar to the surface of LEH their circulation time may be significantly increased. Of greatest interest in this program will be the prospects for better "surface tailoring" of the liposomes to assure that their outermost surfaces are entirely "compatible" with all of the human body's other tissues — platelets, clotting proteins, liver, spleen, and kidney clearance systems, and immunologic defenses. An FY90 Advanced Technology Demonstration (ATD) has been awarded to the Naval Medical Command for a three years advanced development endeavor to transition the

LEH technology base concept to preclinical human trials, the last stage of this exciting Navy-sponsored effort. Preclinical human trials will be conducted in accord with the requirements of the FDA's medical devices regulations.

At that time, the complete transfer of this exciting and new technology, with its enormous potential benefits for public health at large, will require the participation of the private industrial sector. With the successful completion of this technology transfer, the U.S. Navy will have met its own important needs and obligations to its defense personnel, and provide synthetic red blood cell advances that promise a safer, less costly, purer transfusion fluid for the general public than has ever before been available.

Biographies

CAPT. Baier is co-director of the Industry/University Center for Biosurfaces at State University of New York at Buffalo. His research and publications are primarily in biomaterials, surface science, and biological surfaces. He is a member of the Naval Research Laboratory Naval Reserve Unit, Rochester, New York.

CDR Contreras is the Technology Area Manager for Biomedical and Chemical, Biological and Radiological Defense and Deputy Director of the Support Technologies Directorate at the Office of Naval Technology. CDR Contreras, a Ph. D. physiologist, is known for his research and publications in the field of blood and blood substitute research. CDR Contreras has been instrumental in establishing the scope and direction of the Navy's blood research and development efforts.

☆ U.S. GOVERNMENT PRINTING OFFICE: 1989 – 248-783 – 814/00736

Tech Base Notes

Described below is a synopsis of recent technology accomplishments sponsored by the Office of Naval Technology, which is the Navy research and development (R&D) organization responsible for conducting the exploratory development (6.2 category) for the Navy. Exploratory development programs are conducted in industry, academia and in the Navy's own R&D centers.

Recoilless Propellant – Embedded Anchor (RPEA).

To reduce the cost and complexity associated with Fleet and construction moorings, as well as those for certain salvage, diving construction and amphibious operations, the Naval Civil Engineering Laboratory has developed a 20-kip RPEA. This system eliminates the need for cumbersome and expensive piles and deadweights that are presently used for fixed-point uplift-resisting anchors. During tests sponsored by the Office of Naval Technology, the 1-ton RPEA gun system fired a 400-pound anchor 10 to 40 feet into dry ground. The RPEA will save money by reducing the amounts and sizes of support vessels, connective gear and equipment, the time periods and difficulties of mobilizations/installations, and the number of people needed during construction and salvage operations.

Disbond/Delamination Detector.

A low-cost, portable, battery-operated device which detects minute surface perturbations indicating disbonds or delaminations in composite aircraft structures was developed under Office of Naval Technology sponsorship by the Naval Air development center. This provides the Navy with a capability to detect foreign body impact and fatigue damage in the field, thereby helping to prevent catastrophic failures. This effort was recognized at the Second Navy IR&IED Symposium as the Best Independent Exploratory Development Paper of 1989. A patent application is being negotiated, and interest in this technology has been expressed by the international community, as well.

DEPARTMENT OF THE NAVY
OFFICE OF NAVAL RESEARCH
ARLINGTON, VA 22217

OFFICIAL BUSINESS
PENALTY FOR PRIVATE USE, $300